Light Water Reactor Sustainability Program

Production of Fischer-Tropsch Synfuels at Nuclear Plants

September 2022

U.S. Department of Energy

Office of Nuclear Energy

Production of Fischer-Tropsch Synfuels at Nuclear Plants

Daniel Wendt, Marisol Garrouste, William D. Jenson, Qian Zhang, Tanveer Hossain Bhuiyan, Mohammad Roni, Frederick Joseck, and Richard Boardman

September 2022

Idaho National Laboratory
Light Water Reactor Sustainability Program
Idaho Falls, Idaho 83415

Page intentionally left blank

EXECUTIVE SUMMARY

A case study analysis was performed to evaluate nuclear-powered synthetic fuel production in the midwestern United States (U.S.). A Fischer-Tropsch (FT) fuel synthesis plant design was used as the basis for the analysis. The FT plant design was configured to produce a product slate consisting of diesel fuel, jet fuel, and motor gasoline blend stocks from carbon dioxide (CO_2) and hydrogen (H_2) feedstocks. The CO_2 feedstock for the FT plant was assumed to be sourced from biorefineries in the region around a Midwest light water reactor (LWR) nuclear power plant (NPP). The analysis specifies that power from the LWR is used to produce H_2 via high-temperature steam electrolysis and to operate the FT synfuel production plant.

Capital costs were estimated for the FT plant while capital costs for the electrolysis plant were based on previous Idaho National Laboratory (INL) studies. In addition to labor and maintenance costs for the FT and electrolysis plants, operating costs also include the costs for CO_2 feedstock transport. An analysis was performed to determine the cost of transporting CO_2 from the distributed biorefinery sources to the centralized fuel synthesis plant as a function of the synfuel plant capacity and corresponding CO_2 demand. The primary revenue streams are associated with sales of the synthetic fuel products. The synthetic fuel products will likely follow the same market trends as the conventional fuel products. The synfuel price data was thus based on projections made by the U.S. Energy Information Administration (EIA) 2021 Annual Energy Outlook (AEO) for conventional fuel products minus federal and state taxes, as well as marketing and distribution costs. The economic analysis also considered cases that included and excluded revenues from the 2022 Inflation Reduction Act (IRA) clean hydrogen production tax credit (PTC) of $3.00/kg for the first ten years of operation.

The economic analysis calculated the net present value (NPV) for cases involving steady-state synfuel production for comparison with the NPV for a business-as-usual case in which NPP continues to sell only electric power to the grid. A synfuel production "Reference Case" was considered in addition to sensitivity cases in which the plant capacity, electricity price, and synthetic fuel product prices were perturbed. The synfuel production Reference Case considered a scenario in which the electrolysis and synfuel plants utilized a combined electrical load of 1000 megawatt electrical (MWe) from the LWR with the balance of the LWR power output being sold to the electric grid.

The economic analysis suggests that the synfuel production Reference Case evaluated in this analysis would lead to considerable economic potential for near-term deployment of a nuclear-based synfuel production plant. Specifically, the economic analysis suggests that the deployment of a 1000 megawatt (MW) nuclear-powered synfuel plant could result in a NPV increase of approximately $1.7 billion for a case with no clean synfuel price premium relative to conventional petroleum fuels when accounting for the additional revenues from the 2022 IRA clean hydrogen PTCs of $3/kg, as observed in Figure ES-1.
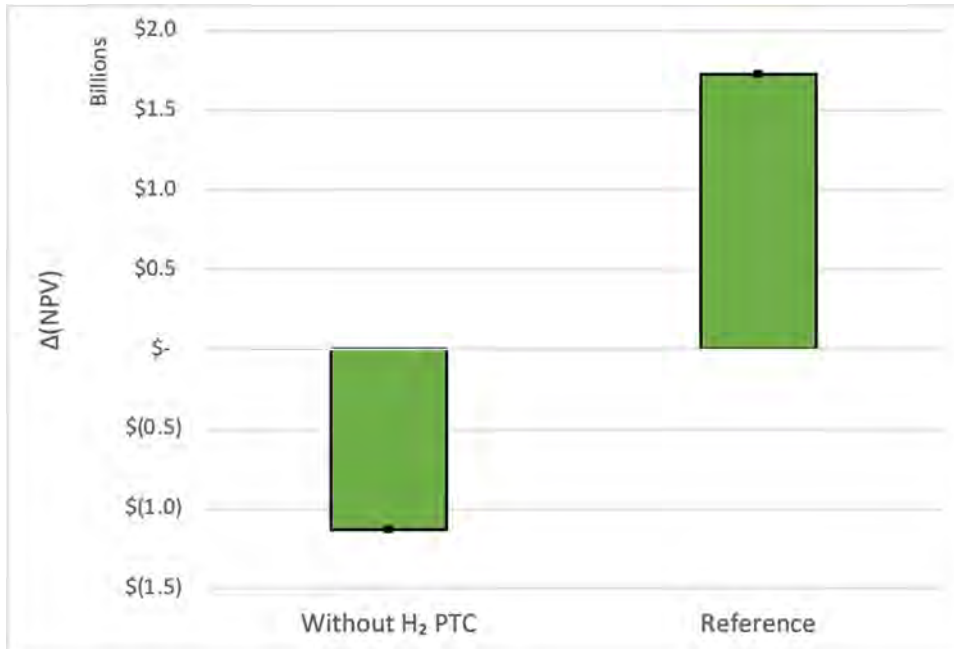
Figure ES-1. Synfuel production Reference Case without and with the 2022 IRA clean hydrogen PTC.

Sensitivity analysis was performed to evaluate the effect of perturbation of selected model input parameters on the NPV for the synfuel production Reference Case, as can be seen in Figure ES-2. The sensitivity analysis indicates that the plant capacity has the largest impact on the differential NPV, with a smaller synfuel production capacity resulting in a decrease in revenue when a larger fraction of the power from the NPP is sold to the grid and a smaller fraction of the power is used to produce synthetic fuel products. The synfuel product pricing has the next largest impact on the differential NPV, with lower synfuel prices resulting in decreased NPV from decreased synfuel sales revenue while higher synfuel prices result in increased NPV from increased synfuel sales revenue. Electricity pricing has a smaller effect on the NPV than the fuel sales price since, in the Reference Case, most of the energy from the NPP is used for synfuel production and a smaller amount of the system revenues are associated with electrical power sales. However, the electricity price sensitivity does indicate that the Synfuel Integrated Energy System (IES) would have a greater NPV than the business-as-usual case (e.g., grid power sales only) when electricity market prices are low, **suggesting that synfuel production could provide a strategy for decreasing the economic risks to NPPs posed by a loss of revenues attributed to falling electricity market prices.**
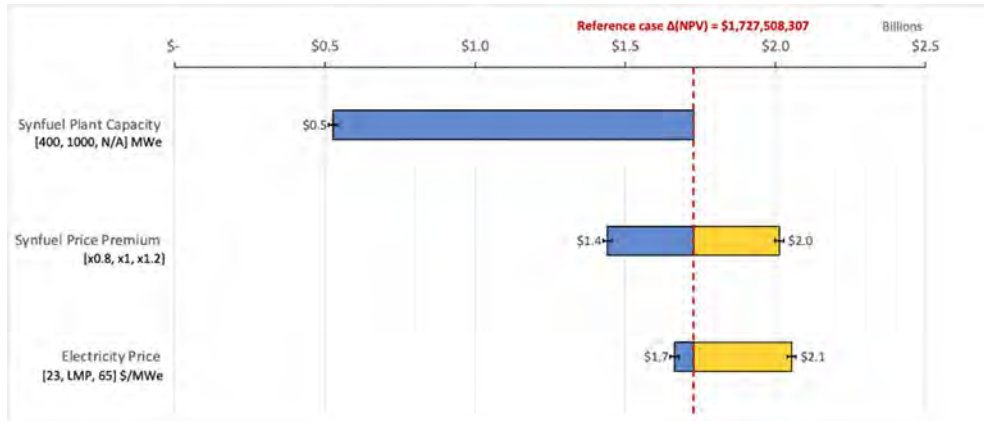
Figure ES-2. Nuclear-based synfuel production sensitivity analysis. The synfuel production Reference Case corresponds to a 1000 MW Synfuel IES, synfuel prices equal to those projected for conventional fuels in the EIA 2022 AEO, residual electrical power sold to the grid at a price consistent with the historical locational marginal price (LMP) at the NPP node, and the inclusion of 2022 IRA clean H_2 PTCs.

Page intentionally left blank

CONTENTS

FIGURES

TABLES

Page intentionally left blank

ACRONYMS

AEO	Annual Energy Outlook
API	Application Programming Interface
ARMA	Auto-Regressive Moving Average
BoP	balance-of-plant
bpd	barrels per day
BMT	billion metric tons
CAGR	compound annual growth rate
CAPEX	capital expenses
CO_2	carbon dioxide
DOE	U.S. Department of Energy
EIA	U.S. Energy Information Administration
EU	European Union
FERC	Federal Energy Regulatory Commission
FT	Fischer-Tropsch
GW	Gigawatt
GHG	greenhouse gas
H_2	hydrogen
HERON	Heuristic Energy Resource Optimization Network
HTSE	high-temperature steam electrolysis
IES	Integrated Energy System
INL	Idaho National Laboratory
IRA	Inflation Reduction Act
ISO	independent system operator
LMP	locational marginal price
LWR	light water reactor
MMBtu	Million British Thermal Units
MMT	million metric tons
MOU	memorandum of understanding
MSTL	Multiple Seasonal-Trend decomposition using Loess
MTG	methanol-to-gasoline
MW	megawatt
MWe	megawatt electrical
MWh	megawatt hour

MWth	megawatt thermal
NEI	Nuclear Energy Institute
NETL	National Energy Technology Laboratory
NOAK	nth-of-a-kind
NPP	nuclear power plant
NPV	net present value
NRC	U.S. Nuclear Regulatory Commission
NREL	National Renewable Energy Laboratory
O&M	operation and maintenance
O_2	oxygen
OSRM	Open Street Routing Machine
PTC	production tax credit
RAF	Royal Air Force
RAVEN	Risk Analysis Virtual ENvironment
RT-LMP	real-time locational marginal price
RTO	Regional Transmission Organizations
RTM	real-time market
RTO	regional transmission organization
SAF	sustainable aviation fuel
SOEC	solid oxide electrolyzer cell
TCI	total capital investment
TDL	thermal delivery loop
U.K.	United Kingdom
U.S.	United States
UAL	United Airlines
USAF	U.S. Air Force
VARMA	Vector Auto-Regressive Moving Average
WACC	Weighted Average Cost of Capital
WEF	World Economic Forum

PRODUCTION OF FISCHER-TROPSCH SYNFUELS AT NUCLEAR PLANTS

1.   INTRODUCTION

In 2021, the United States (U.S.) consumed petroleum products including gasoline, jet fuel, and diesel at a rate of 19.8 million barrels per day (bpd). The transportation sector represents the largest use of these petroleum products, consuming 13.3 bpd of petroleum products (67% of the total U.S. petroleum consumption) [1]. The combustion of petroleum-based fuels releases carbon dioxide (CO_2) into the atmosphere. The U.S. transportation sector was responsible for 1.8 billion metric tons (BMT) of CO_2 emissions in 2021, 97% of which resulted from the combustion of petroleum fuels. The transportation sector carbon emissions represent 37% of the 4.9 BMT total CO_2 emissions in the U.S. [2]. Transitioning to alternative, lower CO_2-emitting, energy sources in the transportation sector could significantly reduce overall CO_2 emissions. While the electrification of light-duty transportation vehicles is an approach that could have significant impacts, aviation, marine, rail, and heavy transport vehicles are not readily converted to electric energy sources due to the lack of availability of batteries that can provide the required quantities of energy storage at an economical price.

Synthetic fuels, which can be used as drop-in replacements for conventional transportation fuels, can be produced from carbon and hydrogen chemical building blocks. If the synfuel hydrogen (H_2) feedstock is produced from a CO_2 emissions-free energy source and the CO_2 feedstock is sourced from the atmosphere, or a biogenic carbon source for which the ultimate source of the carbon was CO_2 from the atmosphere, the use of synfuels could result in a significant reduction in the net CO_2 emissions from transportation applications that would otherwise be challenging to decarbonize. Using drop-in synthetic fuels with a low-carbon footprint also has the advantage of requiring minimal modifications to existing aviation/marine/rail/heavy transport vehicles and the associated fuel transport and delivery infrastructure.

Nuclear power plants (NPPs) represent a low-carbon power source that could be used to produce the H_2 needed as a feedstock for synthetic fuel production, as well as for powering the synthetic fuel production plant. H_2 would be produced from electrolysis that utilizes near-zero carbon power from an NPP. The current fleet of NPPs is distributed across the country, with a large number of them located in the Midwest in relatively close proximity to ethanol biofuel production plants that provide a concentrated biogenic CO_2 source. While existing light water reactors (LWRs) are currently being used to provide electrical power to the grid, there may be opportunities to use nuclear power produced during off-peak times to power synfuel production operations. Additionally, several NPPs have shut down in recent years as a result of being unable to compete in electricity markets where prices have declined due to a large uptake in low-cost wind and solar power; however, for similar cases that may arise in the future, existing NPPs could possibly operate independently of the grid to provide a clean and reliable dedicated source of power for producing low-carbon synfuels.

Several different synthetic fuel production pathways exist. These pathways include the Fischer-Tropsch (FT) process (e.g., hydrocarbon chain growth reactions), the methanol-to-gasoline (MTG) process (e.g., methanol dehydration), hydrogenation processes (e.g., coal liquefaction), pyrolysis processes (e.g., thermal decomposition), bio-oil processing (e.g., deoxygenation, hydrocracking, isomerization), etc. This analysis includes an initial assessment of the economics of producing synthetic fuels using the FT process powered by an LWR NPP. The study considers a scenario based in the Midwest U.S., in which CO_2 from corn ethanol plant surrounding an existing LWR NPP is transported to the NPP site and into a co-located FT-based synfuel production process. The scenario considers use of H_2 produced via a high-temperature steam electrolysis (HTSE) process that utilizes both electrical power and thermal energy from the NPP. In addition to the power requirements associated with H_2 production, the synfuel production process uses power from the NPP to power the FT plant (e.g., powering pumps, compressors, etc.).

2.   SYNFUEL MARKET ANALYSIS

The Biden administration provided incentives and goals to supply three billion gallons of sustainable aviation fuel (SAF) by 2030 and 75 billion gallons per year by 2050 through fuel tax credits [3]. Various projections have been made about SAF growth. These projections for domestic and international synthetic jet fuel result in a compound annual growth rate (CAGR) of 50–60% annually. Traditional aviation fuel needs are expected to grow by 75 billion gallons per year by 2050. Assuming there would still be a need to blend synthetic fuels with traditional fuels, there would be a significant need for an increased supply of synthetic versions of aviation fuel. Demand and supply would both increase significantly as approval is gained for 100% synthetic drop-in fuel as a replacement for traditional fuel. Boeing committed to make aircraft capable of using 100% synthetic fuel by 2030 [4]. A recent study published by the U.S. Department of Energy (DOE) indicated that the global commercial jet fuel market was projected to grow from 106 billion gallons in 2020 to over 230 billion gallons by 2050.

Initial efforts to discover market demand for synthetic naphtha did not yield as many results as SAF. One industry expert indicated that synthetic naphtha may sell for a lower price than traditional naphtha based on quality characteristics. A report from Future Market Insights did suggest that the renewable naphtha market would increase from $422 billion in 2021 to $1.15 trillion by 2031 with a CAGR of 10.5% [5]. The main driver behind the growth is stemming from increasing demand for eco-friendly versions of synthetic plastics. According to the report, 72.8% of global naphtha sales would be used for ethylene and propylene crackers to produce plastics by the end of 2031.

The U.S. diesel market is expected to grow from $935 billion in 2020 to nearly $1.27 trillion by the end of 2027 according to Globe News Wire [6]. The industry is expected to yield a 4.4% CAGR over the same time period. Like aviation fuel, synthetic diesel fuel is a drop-in substitute for traditional fuel with the added advantage of having practically zero sulfur content [5]. Existing engines do not require modifications to accept the synthetic alternative. If cost-competitive synthetic versions of diesel fuel were available, there would be a very large market for the product. According to a McKinsey & Company report on the global energy landscape, sustainable fuels could take up a 37% share of transportation energy demand by 2050 [7]. The report also states that the adoption of electric vehicles might impact the market for internal combustion engine vehicles after 2035. At that point, the demand for sustainable fuel for road transportation may begin to decrease. At the same time, the demand for SAF will likely continue to increase.

2.1   Synfuel Applications

Synfuels can be used for multiple applications because of their ability to 'drop-in' as a substitute for traditional fuels. According to the U.S. Energy Information Administration (EIA), about 28% of total U.S. energy consumption in 2021 was the result of transportation of either goods or people [8]. More than half of this transportation fuel was gasoline, followed by distillates, which includes diesel, and jet fuel. These three forms of fuel combine to make up 88% of U.S. transportation fuel sources, as can be seen in Figure 1. All three of these traditional fuels can be replaced with synthetic versions although synthetic gasoline is typically produced using a methanol synthesis process. Although the market is small, biofuels made up 5% of transportation energy sources, according to the EIA. Interest related to meeting goals set by the 2050 Paris Agreement and the U.S. Long-Term Strategy for net-zero greenhouse gas (GHG) emissions will likely contribute to the increased adoption of synthetic fuels [9].
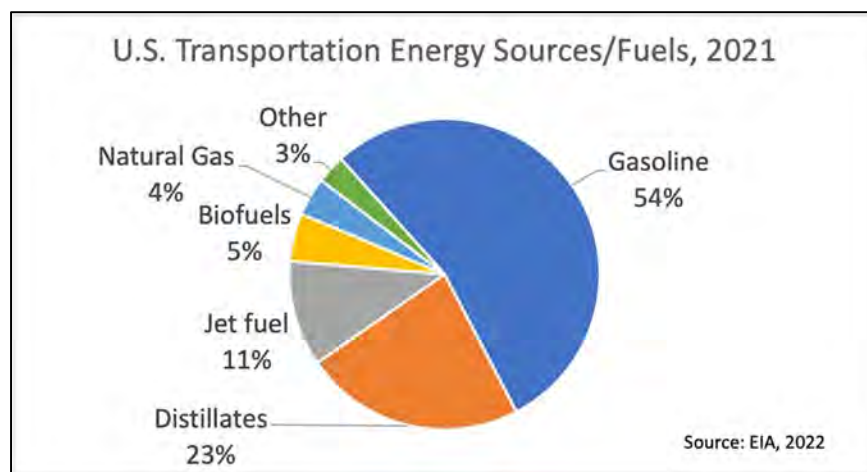
Figure 1. U.S. transportation sector 2021 fuel usage.

2.2   Synthetic Fuel Market Case Studies

While the market for synthetic fuel is still in development, there are cases where these fuels are making steps toward notable applications. In the European Union (EU), Royal Dutch Shell is taking the initiative to develop a synthetic jet fuel production site next to the Forsmark NPP in Sweden [10]. The plant would be operated by Vattenfall AB and LanzaTech, Inc., and would provide up to 25% of the demand for synthetic fuel for the Scandinavian airline, SAS AB. The plant would be operational between 2026 and 2027 and capable of producing up to 50,000 tons of synthetic jet fuel a year. LanzaTech will follow an alcohol-to-jet fuel process. The goal for Vattenfall is to provide the location with fossil-free electricity, hydrogen production, and CO_2 recovery.

In the United Kingdom (U.K.), the Royal Air Force (RAF) flew a 100% synthetic fueled flight in November 2021 [11]. This flight was a step toward eliminating a reliance on fossil fuels. The RAF partnered with Zero Petroleum to test scalability and efficiency of synthetic fuels. The U.K. Ministry of Defence is committed to making the RAF a net-zero operation by 2040 [12]. As part of that effort, the RAF has plans for a net-zero airbase by 2025.

The U.S. military is also looking at synthetic fuels to reduce its carbon footprint. The U.S. Air Force (USAF) created an Energy Flight Plan that outlines energy goals for 2017 through 2036. The document indicated that the USAF has certified its entire fleet to use alternative fuels. The fuels include FT-processed synthetic fuel and a biofuel made by hydroprocessing esters and fatty acids. Initially, these fuels will be mixed at a 50% ratio with traditional JP-8 or Jet A fuel [13].

The USAF plan also makes it clear that the military does not have ambitions to produce the fuels on their own. The USAF plans to work with private companies to meet fuel demands and is currently soliciting suppliers if they can meet cost, environmental, and technical specifications. In 2021, USAF Operational Energy launched a program and endorsed Twelve, a synthetic fuel producer [14]. The entrance of the U.S. military into the market for aviation fuel is significant. Currently, the USAF consumes 10% of the nation's aviation fuel.

There are multiple commercial airlines forming partnerships with and investing in private SAF companies. United Airlines (UAL) and Honeywell joined together in a multimillion-dollar investment in Alder Fuels. UAL agreed to purchase 1.5 billion gallons of SAF over a 20-year period [15]. Alder will combine the use of forestry and agricultural residues with Honeywell's Ecofining process to make the fuel. Alder has been researching SAF production through support of the U.S. Defense Logistics Agency and DOE's National Renewable Energy Laboratory (NREL). Table 1 shows a selection of other airline and SAF producer relationships.

Table 1. Airline and SAF producer relationships.

Airline and SAF Producer Relationships			
Airline	**Producer**	**Quantity (gal)**	**Price**
UAL	Alder	1.5 billion	-
JetBlue	SG Preston	-	>$1 billion
Alaska Airlines	Twelve	-	3-5x Traditional
Delta Airlines	Aemetis	-	$1 billion
JetBlue	World Energy	1.5 million*	-
USAF	Twelve	-	-
*Blended			

2.3   Synthetic Fuel Market Size

The DOE–Office of Energy Efficiency & Renewable Energy (2020) report on SAF indicated the global market demand for commercial jet fuel would increase from 106 billion gallons in 2019 to over 230 billion gallons by 2050 [16]. The U.S. domestic market alone required 26 billion gallons of jet fuel in 2019. Current ASTM International regulations allow aircraft to blend up to 50% synthetic fuel with traditional fuel.

With the Russian/Ukrainian war and the subsequent sanctions on Russian oil, about 3.5 million bpd of diesel fuel and 1 million bpd of jet fuel has been removed from the market [17]. Over the last five years, several U.S. refineries have shut down with a refining capacity of 1,450,000 bpd of crude oil. As a result, 480,000 bpd of diesel fuel and 200,000 bpd of jet fuel have been removed from the U.S. transportation market [18]. The global diesel market produces 30 million bpd. With the removal of 3.5 million bpd of diesel fuel, the market is faced with a deficit of greater than 10%, which has greatly impacted the overall cost of diesel fuel and jet fuel.

2.3.1   National and International Market

The U.S. Department of Energy, U.S. Department of Transportation, U.S. Department of Agriculture, and several other federal agencies have teamed together on forming the Sustainable Aviation Fuel Grand Challenge [19], which is formalized through a memorandum of understanding (MOU) with the purpose of reducing cost, increasing production, and improving SAF sustainability. The MOU includes a goal to have SAF meet 100% of aviation fuel demand by 2050, which equates to 35 billion gallons per year. The challenge has established a goal of 3 billion gallons of SAF per year by 2030.

In July 2022, the EU recently created rules for aviation fuel that will require blending a 2% minimum of SAF into current kerosene-based fuel by 2025. Originally, the EU was targeting a 63% SAF blend by 2050. Under the new guidelines, the blend will increase to 85% by 2050 [20]. These new additions will now go before member governments and the EU Commission for final approval, which is expected in September 2022. Based on a 2021 report by the World Economic Forum (WEF), it should be noted that EU policies would impact international flights departing EU countries; however, the report is unclear regarding the impact U.S. airports servicing international flights might be [21].

WEF identified 25 announced projects in the EU between 2020 and 2025 with SAF production capacity [22]. According to Bloomberg (2021), one project being proposed is backed by Royal Dutch Shell, Scandinavian airline SAS AB, Vattenfall AB, and LanzaTech Inc. The project would utilize the existing Forsmark NPP for SAF production. The plant would be capable of producing 25% of SAS's needs for SAF by the 2030s. The plant would mix recycled CO_2 with H_2 to produce ethanol, which would be further processed into synthetic jet fuel [10].

2.4   Synthetic Fuel Pricing

New markets, like the market for synthetic fuels, often take time to establish a market price. Based on interviews with industry professionals, the synfuels market is still pricing products according to production costs with margins attached. Over time, transparency in the market, which comes from price competition, will determine an equilibrium price. Prices for some synthetic fuels are currently well above traditional fuel prices with some reports showing synthetic fuels selling for double and up to eight times the price of standard fossil fuel prices [23].

In some scenarios, synthetic fuels sell below market prices of traditional fuels. An interview with one industry expert revealed that in some cases, synthetic products compete equally with traditional fuels; however, in other cases, there are deficiencies that result in lower values. The ability to change equal or higher prices depends on the application the synthetic fuel is being used for. This could be the case with synthetic naphtha.

A report by the American Chemicals Society suggested that the levelized cost of synthetic diesel fuel is between 36% and 230% higher than the wholesale price of traditional diesel [24]. Biofuel prices offer a glimpse of what long-term synthetic fuel prices could look like. Biodiesel sold for roughly 1.15 times the price of conventional diesel between 2007 and 2022 according to data from the EIA. Figure 2 illustrates the long-term price relationship of biodiesel and traditional diesel based on that EIA data.
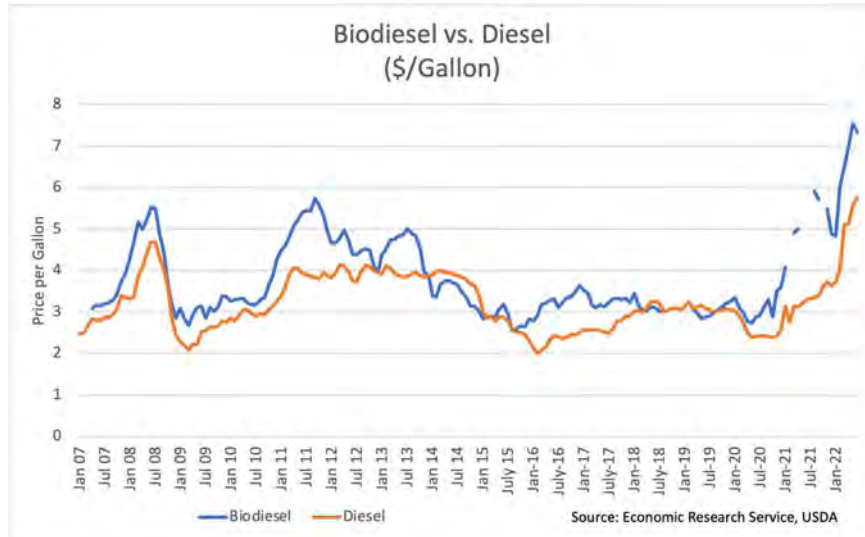
Figure 2. Biodiesel vs. diesel historical prices.

2.4.1   Fuel Price and Demand Projections

Baseline non-synthetic fuel prices for this report were collected from the EIA 2021 Annual Energy Outlook 2021(AEO) report [25]. Price projections were forecasted by EIA through 2050. Fuel price forecasts from EIA were provided in Million British Thermal Units (MMBtu) for gasoline, diesel, and jet fuel. These prices were adjusted converted to dollars per gallon. Once the dollar per gallon conversion was made, it was necessary to remove applicable federal and state taxes that were included in the original price data for all three fuels. The data was further adjusted to remove distribution and marketing markup that would not be applicable to this analysis. Figure 3 shows a breakdown of forecasted traditional fuel prices.
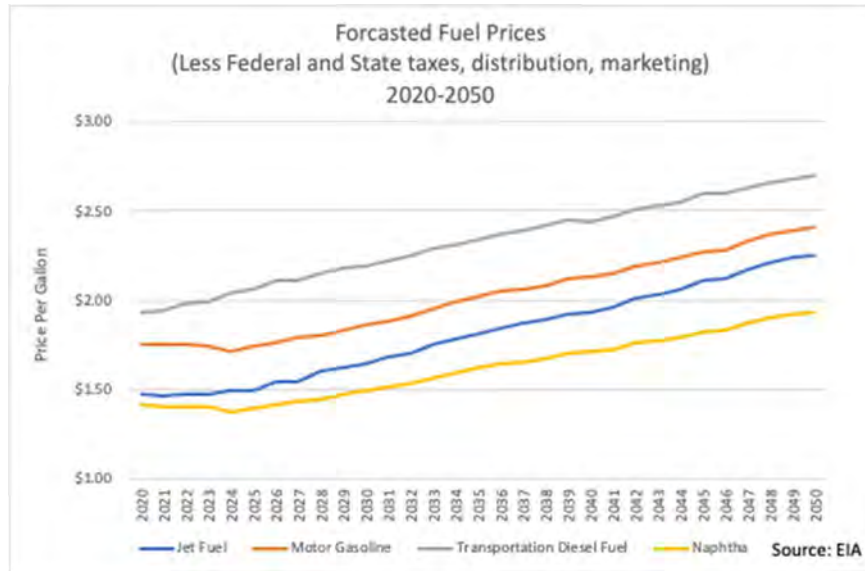
Figure 3. EIA forecasted fuel prices (adjusted).

The adjustment amounts were determined using EIA data. Figure 4 provides a breakdown of typical margins for a gallon of regular grade gasoline. According to EIA, if the retail price of regular gasoline was $3.01 per gallon, roughly 32% of the retail price of gasoline is a result of federal and state taxes, along with distribution and marketing expenses [26].
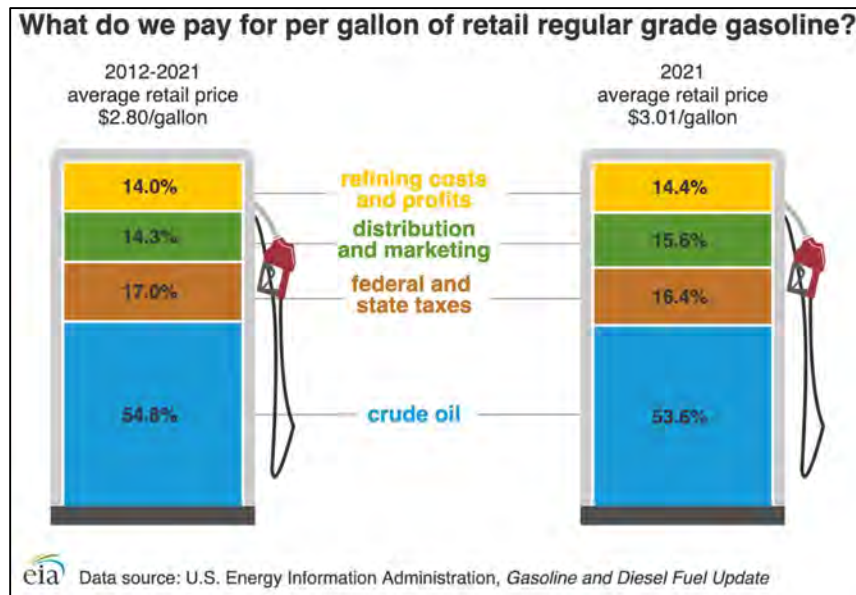
Figure 4. Factors affecting gasoline prices.

Historical naphtha prices showed a strong correlation with gasoline. The correlation coefficient between gasoline and naphtha between 2007 and 2018 was 0.97, but decreased to 0.85 after including data from 2019 through 2022 that was more volatile than in previous years. Naphtha prices per gallon were slightly lower than those observed for gasoline between 2007 and 2022 once taxes, distribution, and marketing expenses were removed. Over this long-term time period, naphtha was typically priced at 0.803 times the price of gasoline. Figure 5 shows the historical relationship between gasoline and naphtha [27].
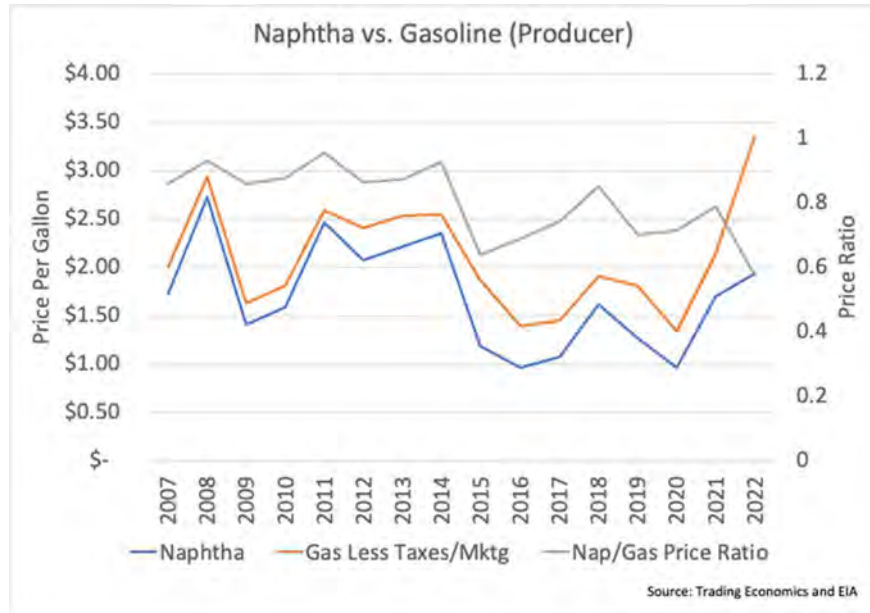
Figure 5. Naphtha vs. gasoline producer price comparison with price ratio.

During the course of completing this report, industry experts were interviewed to provide context for future price expectations. Companies represented during these interviews include Twelve, Dimensional Energy, UAL, and Dakota Gasification Company. Based on discussions with these industry experts, the apparent price premiums placed on synthetic fuel is currently a factor of higher production costs. The market is lacking price information and transparency that will become present once more suppliers enter the market. As mentioned previously, synthetic fuel prices were recently up to eight times the price of traditional fuel prices [23]. For this purpose, the model used in this report allowed for synfuel prices to compare equally with current traditional fuel prices as well as to determine the economic sensitivity of synfuel production to pricing values both lower and higher than traditional fuels.

If net-zero goals become regulations or mandates, the demand for synthetic fuels could keep prices at elevated levels. One industry expert suggested that based on current conditions, prices will remain elevated for the next two or three years.

3. LIGHT WATER REACTOR NUCLEAR POWER PLANT CASE STUDY

3.1 Light Water Reactor Nuclear Power Plant

The Braidwood NPP, which is operated by Constellation Energy, was selected for a case study analysis of nuclear-based synfuel production. The Braidwood NPP is located in northeastern Illinois and includes two Westinghouse 4-loop pressurized water reactors, each with a thermal capacity of 3645 megawatt thermal (MWth). Together, the two units can produce up to 2,386 megawatt electrical (MWe) of clean, carbon-free power. The Braidwood NPP started up in 1987 and the U.S. Nuclear Regulatory Commission (NRC) has granted operating license extensions to 2046 for Unit 1 and 2047 for Unit 2. The Braidwood NPP is shown in Figure 6.

Figure 6. Braidwood NPP in Braceville, Illinois [28].

The Braidwood NPP operates in the PJM Market. This market is deregulated, which means that the price of the power sold by the NPP is determined by market demand and competitive bid prices submitted by other power generators serving this market. This market structure results in competitive wholesale electricity prices that trend higher during periods of elevated (peak) demand and trend lower during periods of low (off-peak) demand.

The Braidwood plant is located in a region where corn ethanol biofuel production is a prevalent industry. The concentrated CO_2 stream that is released from corn ethanol plants could be collected, compressed, and transported to a synfuel plant co-located with the NPP to provide the carbon source necessary for synfuel production. The proximity to a concentrated biogenic feedstock source and the operation of the plant in a deregulated energy market are key attributes that led to the selection of the Braidwood NPP for the case study analysis. Figure 7 gives the locations of ethanol plants and nuclear reactors in the region of interest.
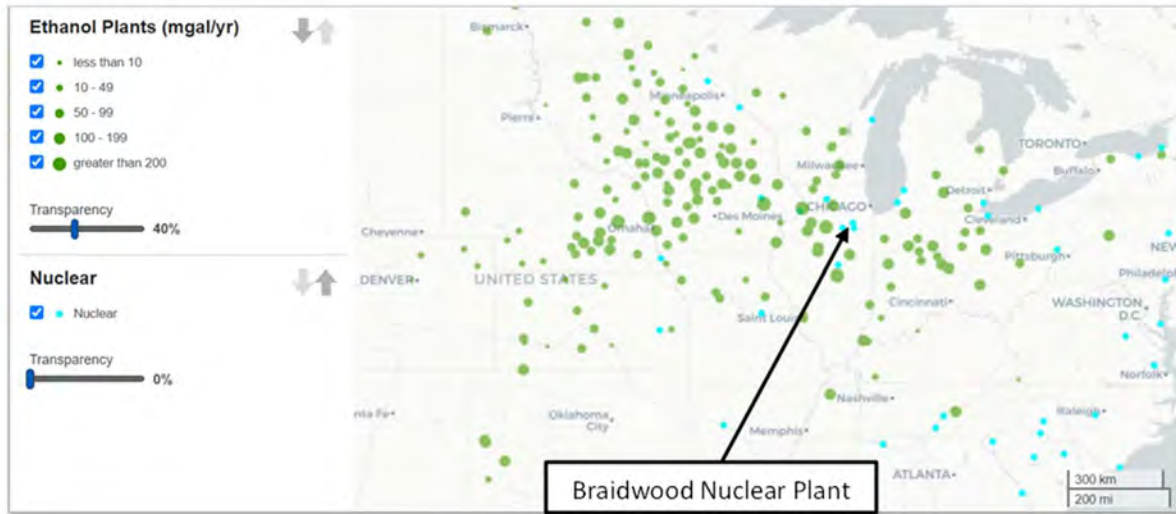
Figure 7. Locations of ethanol plants and nuclear reactors [29].

3.2 Electricity Market Description and Summary of Price Data

3.2.1 Overview of U.S. Electricity Markets

As electricity markets have changed with increases in variable renewable energy within the last few decades, NPPs have been investigating ways to increase profitability, flexibility, and efficiency. One of the potential solutions that have been looked at by researchers is selling electricity to produce commodities such as heat, potable water, hydrogen, or chemical products in addition to selling electricity to the grid. Thus, co-generation systems, including a nuclear reactor, electricity generation turbomachinery, and an industrial process for the production and/or storage of a secondary commodity, have been proposed for currently operating NPPs and next-generation reactors. Figure 8 provides a look at operating NPPs in the U.S. Figure 9 illustrates the mix of fuels used for U.S. electric power generation from 2000 to 2019. Nuclear power has supplied about one-fifth of annual U.S. electricity generation during the past three decades. In 2019, nuclear reactors generated 19% of U.S. electricity supply, behind only natural gas and coal.

Figure 8 shows the nuclear power plants that are operating and under construction in US. Some of these NPPs are integrated with their individual local wholesale electricity markets operated by independent system operators (ISOs) and regional transmission organizations (RTOs), as observed in Figure 8(b). An ISO operates a region's electricity grid, administrates a region's wholesale electricity market, and provides reliability planning for a region's bulk electricity system. RTOs perform the same functions as ISOs, but have greater responsibility for the transmission network as established by the Federal Energy Regulatory Commission (FERC). In addition, as shown in Figure 8(b), there are large sections of the United States, particularly in the Southeast and the West, where there is no ISO or RTO.

Generally speaking, there are two electricity market configurations in the U.S.—regulated and deregulated [30]. In a regulated electricity market, vertically integrated monopoly utilities cover the entire value chain with oversight from a public regulator. The utility makes sure that power is generated, sent to the grid, and reaches customers. Customers in regulated markets cannot choose who generates their power and are bound to the utility in that area. In addition, meeting energy demand at any time involves strategically dispatching the least expensive generation units until the demand is met. This cost-minimization strategy results in a cost to consumers that covers the generation costs. Regulated markets dominate most of the Southeast, Northwest, and much of the West—excluding California, as observed in Figure 10. In a deregulated electricity market, market participants other than utility companies own power

9

plants and transmission lines. In such instances, generators (e.g., companies that generate electricity) sell electricity into a wholesale market, and retail energy suppliers purchase this electricity to sell it to customers. Transmission companies or utilities own and operate the transmission grid. Customers benefit from more competitive rates and generation options, including renewable energy. This market universe is managed by an ISO or RTO. However, it is worth noticing that not all ISO/RTOs operate in deregulated markets; in other parts of the U.S., ISO/RTOs act only as grid operators based on fixed purchase and selling prices.
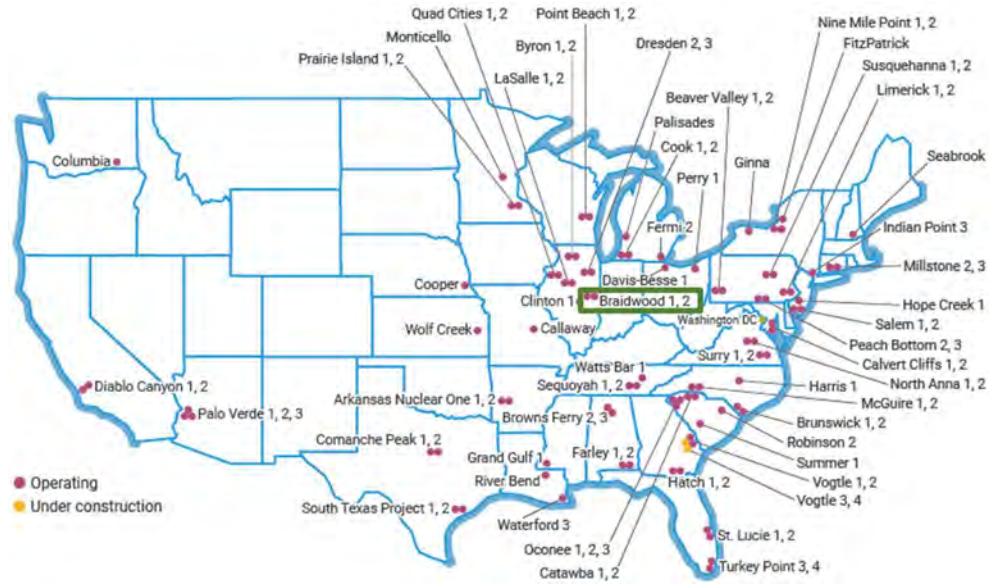
(a)
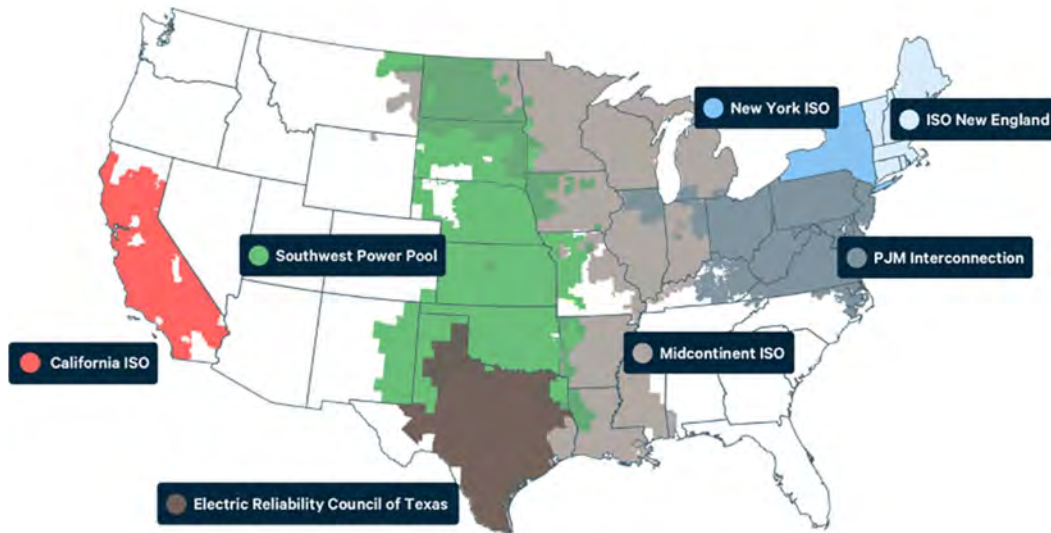
(b)

Figure 8. (a) NPPs operating in the U.S. The green rectangle box indicates the NPP that is considered in this report. (b) ISO/RTO operating power markets in the U.S.
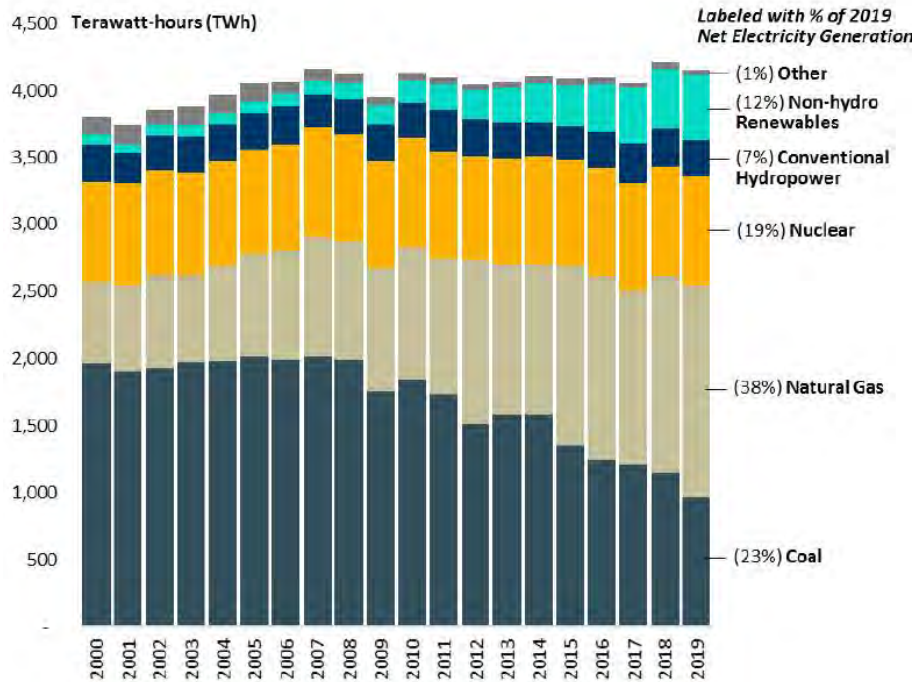
Figure 9. U.S. net electricity generation by fuel from 2000 to 2019.
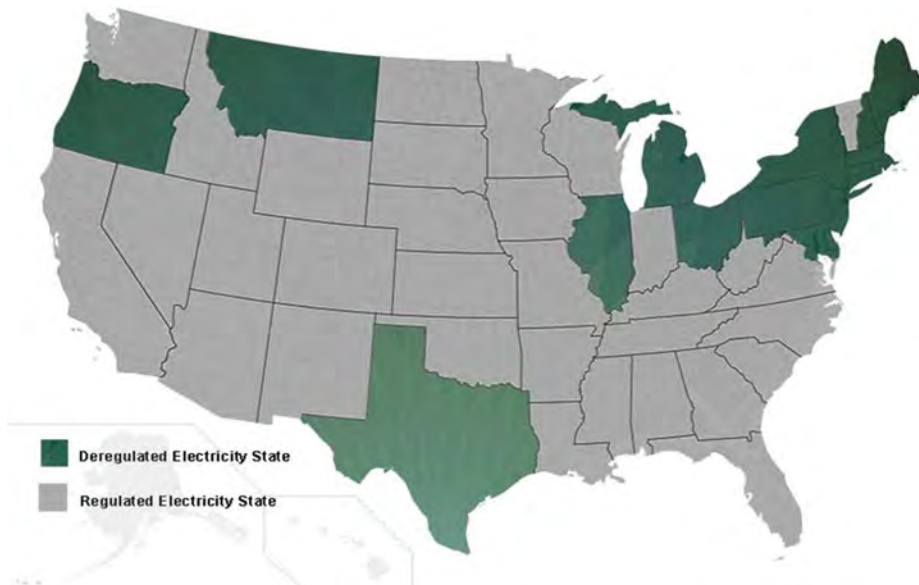
Figure 10. Map of regulated and deregulated markets in the U.S.

3.2.2   Historical Data Analysis in PJM Market

In this report, we focus on the PJM interconnection electricity market that Braidwood NPP is integrating with (see Figure 8 for the location of this NPP). As shown in Figure 10, it is a deregulated market. PJM interconnection operates several types of competitive wholesale markets through which large volumes of electricity are bought and sold across 13 states and the District of Columbia. We are interested in the energy portion of the PJM markets. It is the largest of the PJM markets and makes up the majority of the wholesale electricity costs, which totaled 62% in 2021. The energy market is divided into

the day-ahead and real-time markets. Both match offers from power suppliers with bids from power consumers to ensure that suppliers are ready to deliver at the right time and place. In particular, the real-time market (RTM) serves electricity needs in real-time, which always differs, at least a little, from the day-ahead forecast. The RTM is a spot market, meaning that electricity is procured for immediate delivery. Supply and demand are paired. Real-time locational marginal price (RT-LMP) defines the price for electricity in real-time at specific points referred to as nodes within a transmission system. These prices represent clear benchmark signals for buyers and sellers in electricity markets that provide vital insights in decisions concerning infrastructure investment, enable higher levels of grid stability, and produce competitive markets for reliable power sources.

Figure 11 shows the hourly RT-LMP at the Braidwood node in 2018, 2019, 2020, and 2021 under the operation of PJM interconnection. Before the pandemic, the maximum RT-LMP hits $586.22/megawatt hour (MWh), while the minimum RT-LMP reaches -$25.32/MWh in 2018. In 2019, the maximum RT-LMP hits $690.03/MWh, while the minimum RT-LMP reaches -$52.77/MWh. In the period of the pandemic, the maximum RT-LMP hits $339.16/MWh, while the minimum RT-LMP reaches -$4.94/MWh in 2020. In the year 2021, the maximum RT-LMP hits $542.37/MWh, while the minimum RT-LMP reaches -$16.56/MWh. The annual average of RT-LMP is $35.69/MWh in 2018, $26/MWh in 2019, $20.62/MWh in 2020, and $38.12/MWh in 2021 as observed by the orange lines in Figure 12(b), (d) (f) and (h). In addition, it is easy to see that there are several hours (e.g., 4 hr. out of 8760 hr. in 2018 and 2019, 3 hr. out of 8784 hr. in 2020, and 1 hr. out of 8760 hr. in 2021) within a year with negative values of RT-LMP. This is because the locational marginal price (LMP) value is a calculated combination of the electricity price, congestion on the transmission grid, and line losses. For coal and nuclear plants, it can be time-consuming and expensive to ramp up or down, meaning that they may choose to stay online all day regardless of the price of electricity. Wind and solar resources have a zero-dollar fuel cost, making them almost free to run whenever the sun is shining or the wind is blowing. Wind resources also benefit from federal production tax credits (PTCs) meaning they can often operate economically even while accepting negative prices. Therefore, it is possible for electricity supply to exceed consumer demand in wholesale electricity markets, and in these conditions, prices can go negative. Negative prices are worth an extra look because they represent a strange phenomenon: generators paying, rather than getting paid, to provide electricity. At the Braidwood node, the frequency of negative price events is low at least in 2018, 2019, 2020, and 2021. Therefore, we will not take specific consideration for the negative price events in the electricity market at Braidwood NPP.

In Figure 11, we also include the average cost to operate an NPP ($33.50/MWh) as reported by the Nuclear Energy Institute (NEI) in a 2018 study for reference, as observed by the orange lines in the figure. At all points below the cost to generate the line, the nuclear utility is losing money [31]. This is 67.2%, 88.2%, 93.0%, and 56.7% of the time in years 2018, 2019, 2020, and 2021, respectively, in which the electricity price is below the cost to generate. Through the addition of an HTSE unit, where electricity can fluctuate via the switchyard after the turbine, there is an opportunity for the nuclear facility to reduce hours of negative revenue by selling to the hydrogen market when it is profitable to do so.
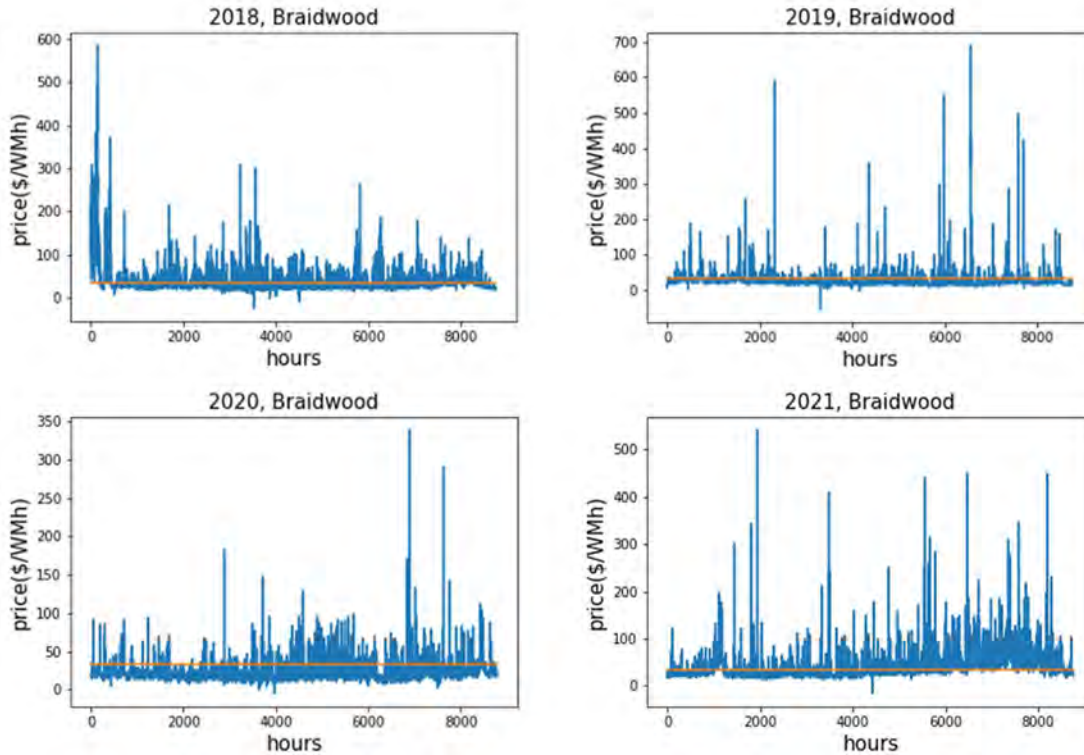
Figure 11. RT-LMPs at Braidwood NPP in 2018, 2019, 2020, and 2021. The orange line represents the average cost to operate an NPP.

Figure 12(a), (c), (e) and (g) provide the letter-value plots showing the statistical distribution of the RT-LMP in each month of years 2018, 2019, 2020 and 2021. The letter-value box is generated for the data of each month with the thickest box in the middle covering the central 50%, while the second box extends from the first to cover half of the remaining area (e.g., 75% overall, 12.5% left over on each end). The third box covers another half of the remaining area (e.g., 87.5% overall, 6.25% left on each end), and so on until the procedure ends and the leftover points are marked as outliers depicted as diamonds. As for the monthly mean value of RT-LMP, January is the month with the highest average electricity price, which was $74.11/MWh in 2018 and $30.64/MWh in 2019, as observed in Figure 12(b) and (d), and is likely associated with the cold weather in the corresponding area. The lowest monthly average electric price was $25.67/MWh in February 2018 and $21.98/MWh in June 2019. The annual average of RT-LMP in 2018 is $35.69/MWh and $26/MWh in 2019 as observed by the orange lines in Figure 12(b) and (d). During the pandemic in 2020 and 2021, the low electricity price is likely associated with the influence of the pandemic on the economy of the country as observed in Figure 12(f). The progressive increase in electricity price from March to November 2021 is likely associated with the reopening policy after the promotion of vaccines as illustrated in Figure 12(h). In addition, comparing the annual average electricity prices of these four years, the highest value is $38.12/MWh in 2021. This is probably because of the high inflation rate after the pandemic (7% in 2021).

We also analyzed the seasonality of the electricity price through these four years. Daily and weekly seasonality of the electricity price are well captured by the Multiple Seasonal-Trend decomposition using Loess (MSTL) algorithm. Detailed discussion and results can be found in Appendix A.

13
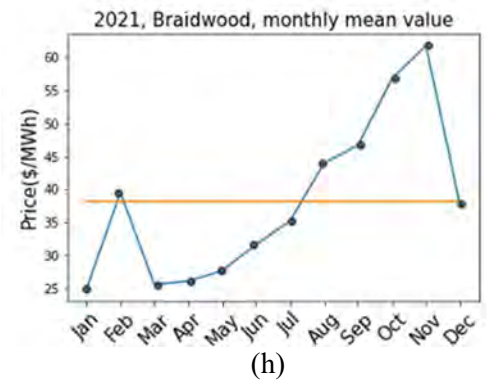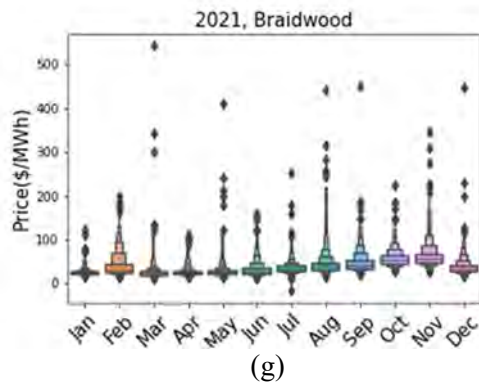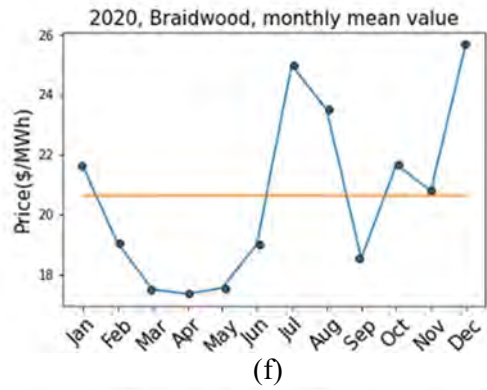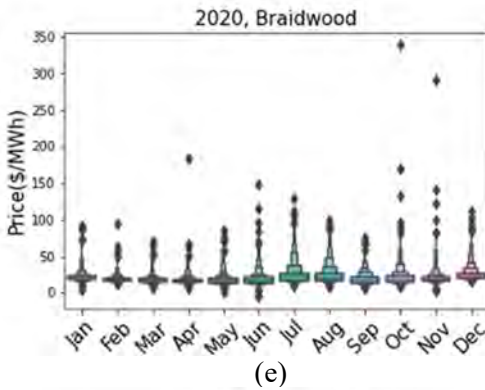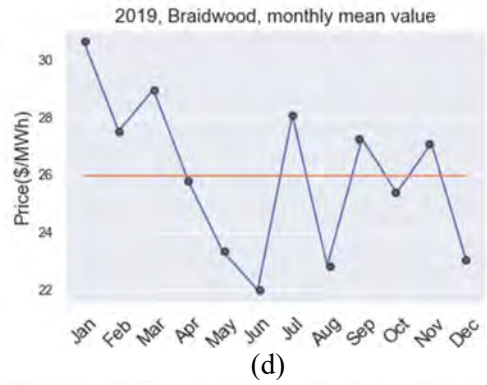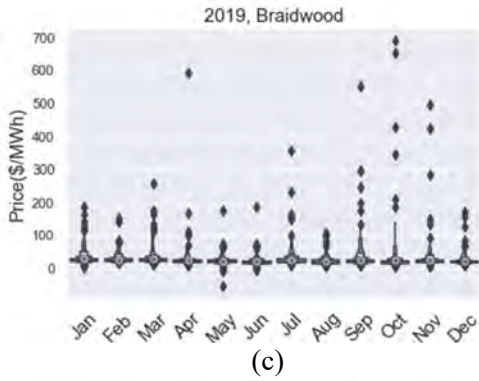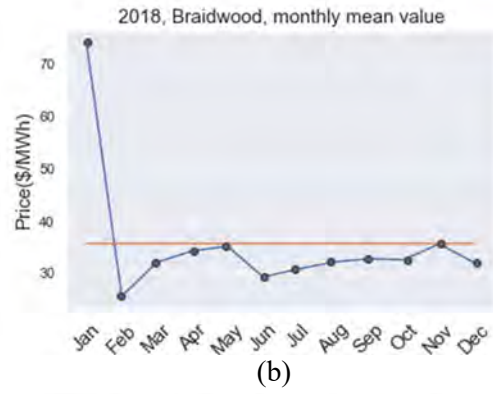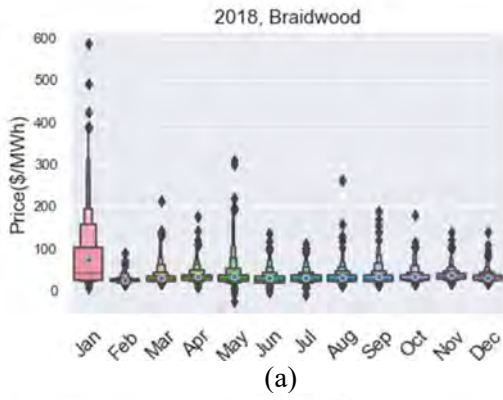
Figure 12. Letter-value plots of duration for the hourly RT-LMP data, grouped by months in (a) 2018, (c) 2019, (e) 2020, and (g) 2021 while the monthly average RT-LMP is shown in (b) 2018, (d) 2019, (f) 2020, and (h) 2021. The orange lines indicate the annual average price for the year 2018, 2019, 2020 and 2021.

3.2.3 Highest and Lowest Electricity Price for the HERON Model Sensitivity Analysis

As the wholesale LMP is expected to be higher in regulated markets as compared with deregulated markets, we use the electricity price in Arizona (regulated market) to estimate the highest value of electricity price within the U.S. However, historical regulated market information is not publicly available. Thus, we estimate the LMP in Arizona with an average monthly industrial bill obtained from the annual report of data from EIA-861 forms. As shown in Figure 13(a), the average monthly price in Arizona is $64.72/MWh for ten years from 2008 to 2018. As for the estimation of the lowest electricity price among the markets we are interested in for this project, we will take the annual average RT-LMP in Houston for reference, as observed in Figure 13(b). This is because the Electric Reliability Council of Texas (ERCOT) is a deregulated market and the natural resource in Texas for electricity power generation is much richer than in the other areas we are interested in for this project. As shown in Figure 13(b), the lowest annual average RT-LMP in Houston is $22.98/MWh from 2011 to 2019.
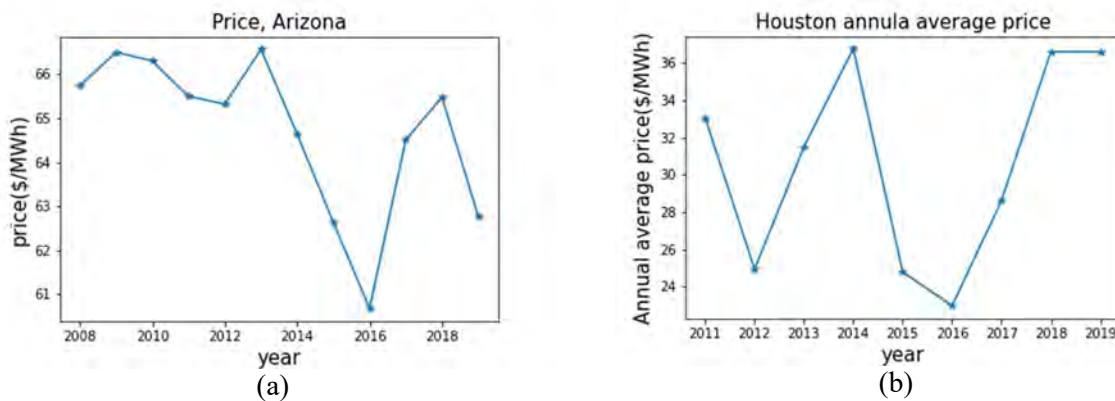
Figure 13. (a) Annual average of monthly industrial electricity bill in Arizona. (b) Annual average of RT-LMP in Houston from 2011 to 2019.

3.2.4 ARMA Time Series for Electricity Pricing

Product price, as well as the weather, are not easily predictable, but they are drivers for optimal resource utilization in any energy system. Treating them as stochastic processes using a sampling approach, the average optimal resource utilization scheme can be computed robustly through the Heuristic Energy Resource Optimization Network (HERON) and Risk Analysis Virtual Environment (RAVEN).

Using the signal analysis capabilities in RAVEN, the generation of synthetic time series is possible. Their behavior will be consistent and they will retain statistical independence [32]. The trends in the periodic data are found and removed from the original signal via Fourier analysis. An Auto-Regressive Moving Average (ARMA) model is then fitted to the residual noise. The Fourier periods are selected to remove consistent periodic signals in the initial signal to detrend it. The ARMA model is then trained on the detrended data to capture noisy deviation from the periodic signal. If the signals are correlated—electricity prices in a market with high renewable penetration and wind speed data for example—the ARMA then is expanded to the Vector Auto-Regressive Moving Average (VARMA) algorithm [33] to capture the correlation between the initial signals.

Figure 14 shows the initial data—electricity prices for the years 2018 to 2021 in the PJM market—and the corresponding data series generated by the trained ARMA model. The time series generated by the ARMA model is not a prediction, and thus, the little overlap between the two series is to be expected. We can observe that the variability and seasonal trends are however roughly the same for the two time series, which indicates the ARMA model produces time series representative of the initial data behavior.
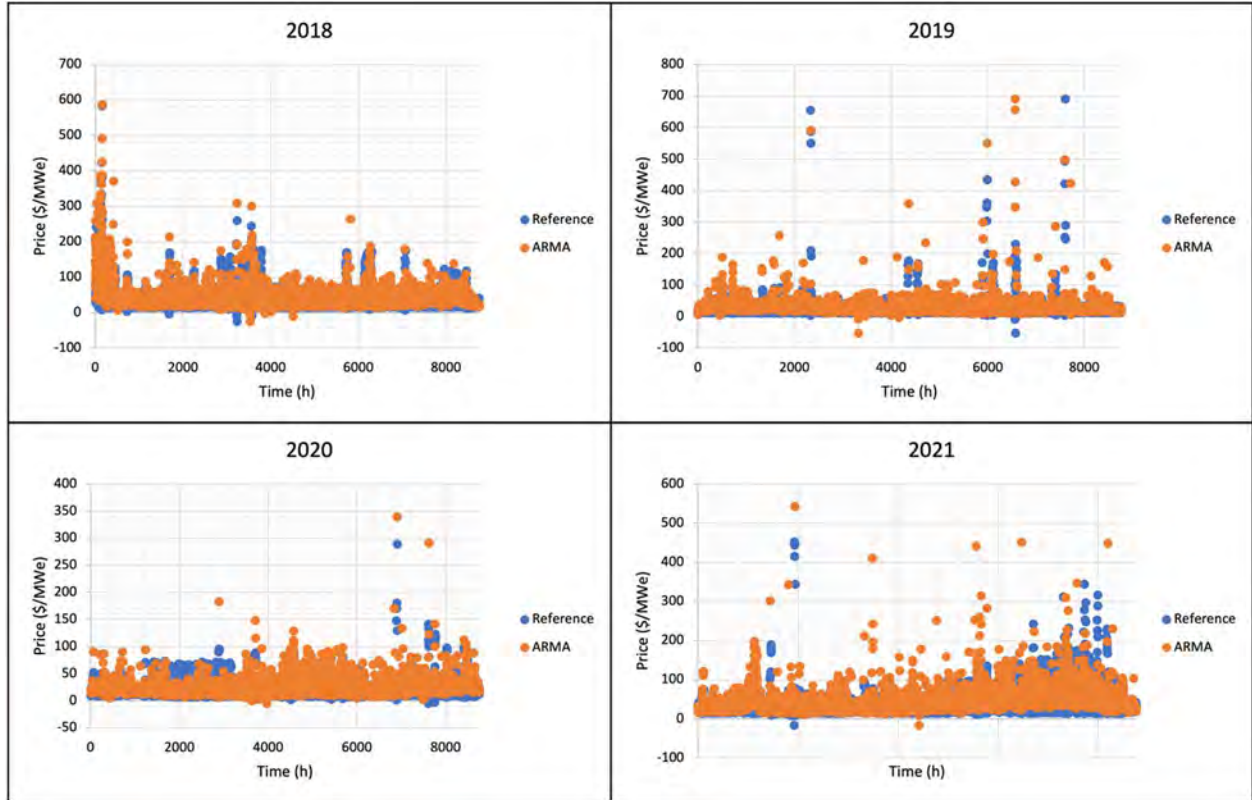
Figure 14. Comparison between initial electricity price for the PJM market at the Braidwood node and projection from the ARMA model for the years 2018 to 2021.

3.3 Fischer-Tropsch Synthetic Fuel Production Process

The FT process is a chemical process that converts a syngas mixture of CO and H_2 into liquid hydrocarbons via catalyzed chemical reactions that take place in the temperature range of 150–300°C. Products from the FT process may include diesel fuel, jet fuel, and lubricants, as well as blendstocks for gasoline fuels.

The FT process produces long chain hydrocarbons through a series of condensation polymerization reactions. Generic equations representing the formation of alkane and alkene products, respectively, are provided in Equation (1) and Equation (2), respectively:

$$(2n + 1) H_2 + n CO \rightarrow C_n H_{2n+2} + n H_2 O \tag{1}$$

$$2n H_2 + n CO \rightarrow C_n H_{2n} + n H_2 O \tag{2}$$

This reaction mechanism results in primarily straight-chain hydrocarbon formation. The use of a cobalt-based catalyst favors alkane production, while the use of an iron-based catalyst favors alkene production [34]. The chain length of the products tends to range from 1 to 20, with the yield of longer chain hydrocarbons favored at lower temperatures (e.g., 220–240°C). The FT naphtha products have a chain length of $5 \leq n \leq 9$, the jet products have a chain length of $10 \leq n \leq 14$, and the diesel products have a chain length of $15 \leq n \leq 18$. FT wax products (n>18) can be cracked to reduce the chain length into the range of the desired fuel products listed above.

The FT process was commercialized in 1936, when Germany used it during World War II to produce liquid fuels from coal. The FT process since has been utilized in numerous other locations for liquid fuel production from coal or natural gas. The largest FT plant in the world is the Sasol Secunda plant located

16

in South Africa, which produces 160,000 bpd of FT liquids from a coal feedstock. As of 2020, this plant was listed as the world's largest single GHG emitter.

However, when CO_2 is used as the carbon source instead of natural gas or coal,[a] and hydrogen is sourced from a process with low-carbon emissions—such as nuclear- or renewable-based electrolysis—the net CO_2 emissions from producing and the use of the resulting drop-in liquid hydrocarbon fuel could be significantly lower than from the production and use of conventional petroleum fuels. If biogenic CO_2 (or CO_2 from the atmosphere), pink/green hydrogen, and zero carbon energy is used in the production of the synthetic liquid hydrocarbon fuels, the resulting synfuels may be carbon neutral.

The current analysis evaluates the economics of FT fuel production using pink hydrogen produced from nuclear-based electrolysis and a CO_2 carbon source sourced from corn ethanol biorefineries located around the synfuel production plant site, which is co-located with the NPP. The analysis was performed in collaboration with Argonne National Laboratory, which developed detailed Aspen Plus process models of the nuclear-integrated FT synthetic fuel production process [34-36]. A block flow diagram of the synfuel production process including the reverse water gas shift reactor to produce synfuel from the H_2 and CO_2 feedstock, FT synthesis reactor, and product purification and recycle are shown in Figure 15 [34].
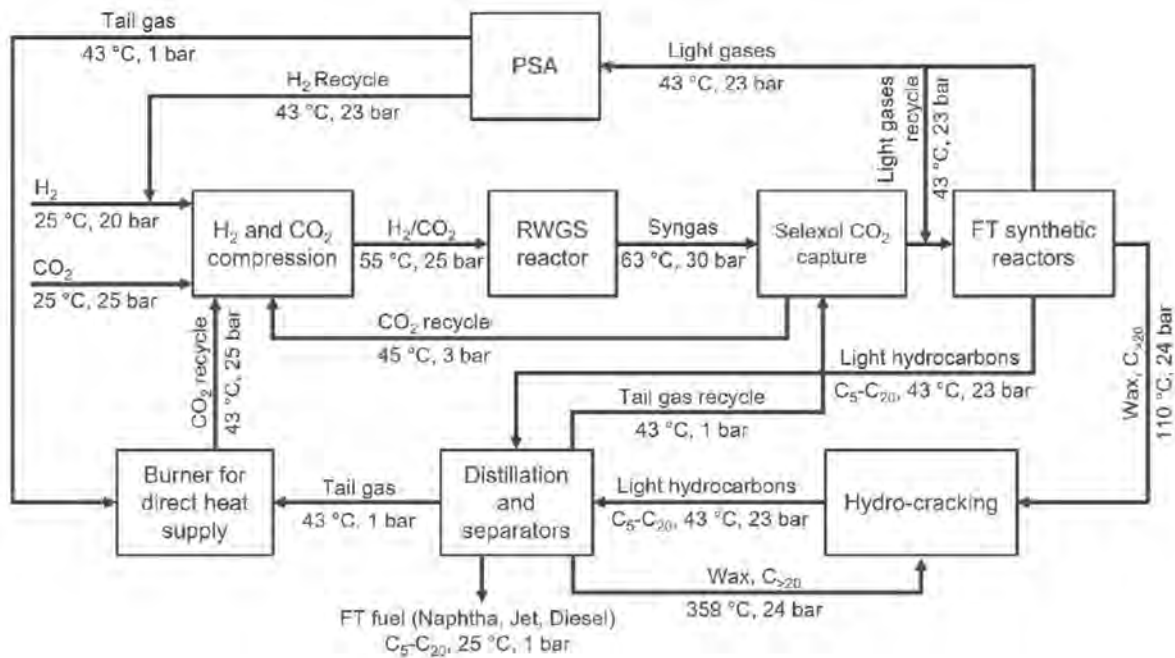
Figure 15. An FT fuel process flow diagram with temperature and pressure values of main streams. The diagram is reproduced here from [34].

Several different FT process capacities are considered in the process and economic analyses. The selected range of the capacities from 100 MWe up to 1000 MWe in the combined power requirement for the electrolysis and FT plants. As the existing fleet of LWR NPPs generally have unit capacities on the order of approximately 1000 MWe, the scale of synfuel plant capacities selected for this analysis corresponds to operating scenarios that would involve approximately 10% up to 100% of the power produced by a LWR unit being used for FT synfuel production. The analysis considers steady-state operation of the electrolysis and FT plants. It is assumed that the balance of NPP power generation

---

a.   The reverse water gas shift reaction may be used to convert CO_2 and H_2 to CO and H_2O, which may be further processed to yield a syngas mixture of CO and H_2 that can be converted to a wide range of potential products including synthetic fuels.

continues to be sold to the electric grid. The feedstock input requirements and synfuel product flow rates for each of the production capacities considered are detailed in Table 2.

Table 2. Feedstock demand and product capacity for different plant scales. Reproduced from [34].

		FT-100	FT-400	FT-1000
Feedstock	H_2 (MT/d)	56	255	601
	CO_2 (MT/d)	348	1,580	3,724
Products	Naphtha (MT/d)	39	176	414
	Jet fuel (MT/d)	47	213	502
	Diesel (MT/d)	26	118	278
	Total FT fuel (gal/d)	40,430	183,030	431,050
Carbon conversion		99%	99%	99%

FT process capacity impacts the economics of synfuel production in several ways. First, as the capacity of the FT plant increases, the required feedstock flow rates also increase. Since water is the primary material feedstock for hydrogen production, and water is assumed to be readily available at the designated synfuel production plant location, the synfuel plant capacity does not have a direct impact on water feedstock cost. However, since the CO_2 feedstock must be obtained from distributed ethanol biofuel production plants in the area surrounding the synfuel production plant, the capacity of the synfuel plant does impact the distance over which the CO_2 feedstock must be transported. As the synfuel production capacity increases, CO_2 must be obtained from a greater number of distributed biofuel plants located at further distances from the centralized synfuel plant. As the length of the CO_2 pipelines that must be constructed to connect additional biofuel plants to the synfuel plant increases, the average CO_2 feedstock cost increases accordingly. The relationship between CO_2 feedstock cost and synfuel plant capacity are addressed in additional detail in Section 3.5.

Second, the synfuel production process capacity impacts the capital costs of the FT plant, as well as the electrolysis plant. The unit capital costs on a $/kW basis of each of these processes is expected to decrease as plant capacity increases due to economies of scale. FT process capital costs are detailed in Table 3, while the electrolysis process capital costs are described in Section 3.4.

Table 3. Detailed capital expenses (CAPEX) for each of the three designed FT plant scales. Reproduced from [34].

	FT-100 (10³ USD)	FT-400 (10³ USD)	FT-1000 (10³ USD)
Direct depreciable capital cost			
H₂ compression	$4,977	$7,761	$14,983
RWGS reaction	$8,487	$19,627	$40,990
CO₂ capture	$6,289	$12,136	$23,428
FT synthesis	$4,759	$11,139	$23,378
Hydroprocessing	$18,739	$47,351	$81,533
Utilities	$4,600	$9,636	$19,619
Total direct depreciable capital cost	**$47,851**	**$107,650**	**$203,931**
Indirect depreciable capital cost			
Site preparation	$957	$2,153	$4,079
Engineering and design	$4,785	$10,765	$20,393
Project contingency	$7,178	$16,147	$30,590
Up-front permitting costs	$7,178	$16,147	$30,590
Total indirect depreciable capital cost	**$20,098**	**$45,213**	**$85,651**
Non-depreciable capital cost			
Land cost	$1,019	$2,293	$4,344
Total capital costs	**$68,968**	**$155,155**	**$293,926**

Finally, synfuel production energy requirements change with plant capacity. Table 4 provides process energy input requirements and product output energy content for each of the selected synfuel production capacities. If the energy price varies with the quantity required (e.g., greater energy demand is correlated with increased price in a similar manner to basic economic theory), then increases in the plant capacity may impact the energy costs incurred by the synfuel process. However, this HERON analysis further described in Section 3.6 assumes a 'price taker' model such that the operation of the synfuel production process does not affect electricity market pricing. Table 4 also reports the calculated process efficiency based on the lower heating value of the product slate. The calculated process efficiency depends primarily on the conversion pathway and process configuration; since the same conversion pathway and process configuration are utilized for each of the plant capacities evaluated in this analysis, the process efficiency is equal for each of the plant capacities evaluated in this analysis.

Table 4. Energy balance and overall efficiency for the combined FT plant-NPP system. The energy values were calculated with respect to the lower heating value. Reproduced from [34].

		FT-100	FT-400	FT-1000
Input	Electric power (H₂ prod.)	86.2	390.9	922.2
	Thermal power (H₂ prod.)	15.0	68.0	160.4
Output	Electric power	3.4	15.5	36.6
	Naphtha	19.7	89.6	210.4
	Jet fuel	24.0	108.7	256.4
	Diesel	13.2	59.9	141.3
	Steam	16.1	73.0	174.6
Total energy efficiency		69.8%	69.8%	69.8%

3.4 Electrolytic Hydrogen Production using Nuclear Power

This analysis considers the use of a nuclear-integrated HTSE process to produce the hydrogen feedstock necessary for synfuel production. Hydrogen production in the HTSE process occurs in a stack of solid oxide electrolyzer cells (SOECs), which operate at high temperatures (e.g., 700–800°C) to increase the efficiency of the HTSE process. In addition to electric power, the HTSE process requires thermal energy input to vaporize the feedwater stream and achieve the required stack operating temperature. The SOEC electrolyte is a solid oxide ceramic material that conducts oxygen ions in a specified operating temperature range. Electric current flows into the cathode where water is split into H_2 (gaseous) and O^{2-} ions. The O^{2-} ions are transported across the electrolyte to the anode where the electric current exits the cell and the O^{2-} ions combine to form O_2 (gaseous) [37]. The SOEC configuration is illustrated in Figure 16. Equations (3) and (4) show the formulas for the cathode and anode, respectively.

Cathode: $H_2O(g) + 2e^- \rightarrow H_2(g) + O^{2-}$ (3)

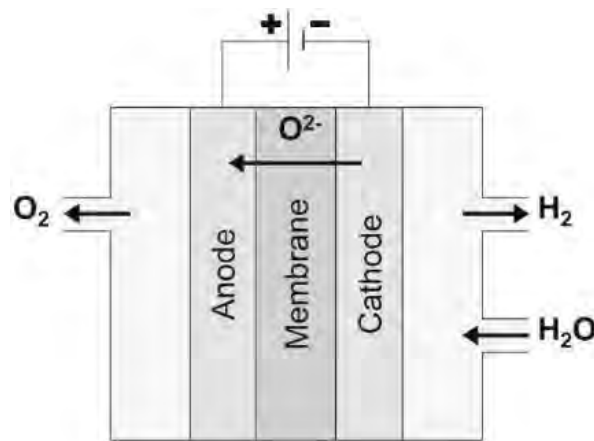Anode: $O^{2-} \rightarrow \frac{1}{2}O_2(g) + 2e^-$ (4)

Figure 16. SOEC configuration. Adapted from reference [38].

To operate the SOEC stack at elevated temperatures, the process requires a balance-of-plant (BoP) configuration with a feedwater steam generator, recuperating heat exchangers (HXs), topping heaters, as well as compressors/blowers to pressurize/circulate the vapor phase reactants and products and the sweep gas used to balance the pressure between the cathode and anode sides of the cells. Additionally, since the H_2 product gas exiting the SOEC stack includes a quantity of unreacted steam, additional process operations are required to remove the water from the H_2 product (e.g., typical water removal steps include cooling/compression and/or pressure swing adsorption).

The NPP provides electrical power to the HTSE process to operate the SOEC stacks, as well as the BoP pumps, compressors, topping heaters, instrumentation, etc. A thermal delivery loop (TDL) is used to transport heat from the NPP to the HTSE plant to provide the thermal energy needed to vaporize the HTSE process feedwater. The TDL is a pipe network that circulates a heat transfer fluid that indirectly transfers heat from the NPP steam to the HTSE feedwater. The TDL enables the NPP and HTSE plant to be located a safe distance apart (e.g., ~1 km), as well as providing physical isolation of the nuclear and non-nuclear systems.

This analysis specifies use of an Nth-of-a-kind (NOAK), modular construction, nuclear-integrated HTSE plant. Since this analysis considers nuclear-based synfuel production at several different capacities, the HTSE plant must be scaled accordingly. The design basis for the NOAK HTSE plant specifications utilized in this analysis are detailed in Idaho National Laboratory (INL) report INL/RPT-22-66117 [39]. Table 5 provides a summary of the HTSE process operating condition specifications. Figure 17 provides a summary of the NOAK modular HTSE plant type total capital investment (TCI) as a function of plant capacity based on a SOEC stack cost of $78/kW-dc corresponding to analysis by James and Murphy [40]. This stack cost is estimated for a SOEC stack manufacturing rate of 1,000 megawatt (MW)/yr. Although SOEC stack manufacturers are currently constructing factories with up to a 500 MW/yr capacity [41], additional time will be required to achieve the 1,000 MW/yr target.

Table 5. HTSE and related subsystem process operating condition specifications.

Parameter	Value	Reference or Note
Stack operating temperature	800°C	O'Brien et al. 2020 [42].
Stack operating pressure	5 bars	See Section 2.2.1 of INL/RPT-22-66117 [39].
Operating mode	Constant V	
Cell voltage	1.29 V/cell	Thermoneutral stack operating point.
Current density	1.5 A/cm²	James and Murphy 2021 [40].
Stack inlet H_2O composition	90 mol%	O'Brien et al. 2020 [42].
Steam utilization	80%	See Section 2.2.1 of INL/RPT-22-66117 [39].
HTSE modular block capacity	25 MW-dc	1000x capacity increase [42].
Sweep gas	Air	O'Brien et al. 2020 [42].
Sweep gas inlet flow rate	Flow set to achieve 40 mol% O2 in anode outlet stream	
Stack service life	4 years	HFTO Hydrogen Production Record 20006 [43].
Stack degradation rate	0.856%/1000 hr.	HFTO Hydrogen Production Record 20006 [43].
Stack replacement schedule	Annual stack replacements completed to restore design production capacity	Based on H2A model stack replacement cost calculations.
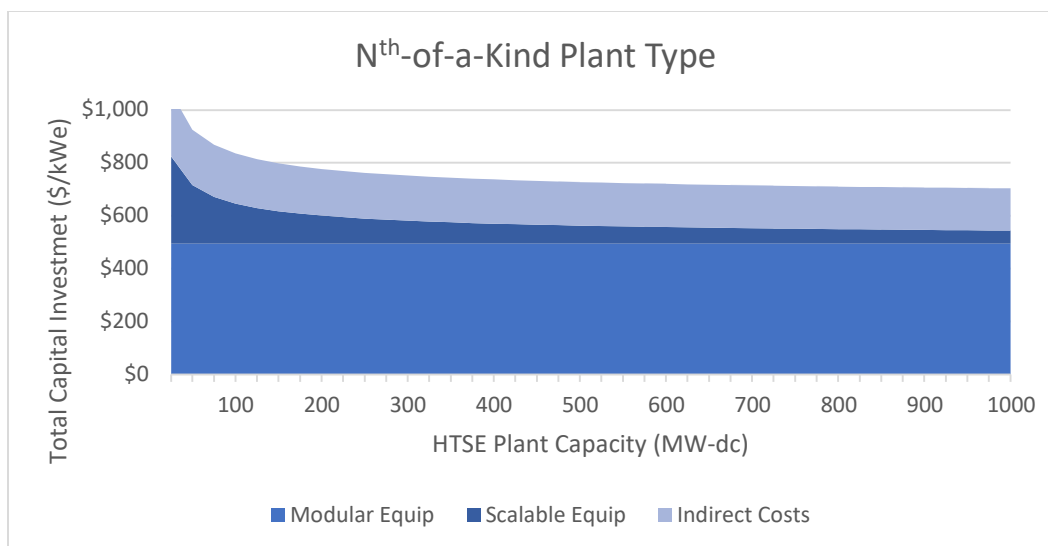
Figure 17. TCI as a function of plant capacity for an NOAK HTSE plant with a stack capital cost specification of $78/kW-dc [40].

Table 6 provides a summary of the NOAK, nuclear-integrated, modular HTSE performance and cost parameters at the capacities considered in the synfuel production analysis. Additional details regarding the HTSE process design can be found in INL/RPT-22-66117 [39].

Table 6. HTSE performance and cost parameters at selected capacities.

	FT-100	**FT-400**	**FT-1000**
H_2 Production Rate (MT/day)	56	255	601
Energy Consumption Electric (MWe) Thermal (MWth)	86.2 15.0	390.9 68.0	922.2 160.4
Direct Capital Cost ($/kW-dc)	665	573	547
Total Capital Investment ($/kW-dc)	861	742	708
Fixed Operating Cost ($/kW-dc-yr)	32.64	32.64	32.64
Variable Operating Cost, excluding energy costs ($/MW-dc-hr)	3.41	3.41	3.41

3.5   CO$_2$ Feedstock Supply Curve

This analysis considered CO_2 from ethanol biorefineries as the primary carbon source for synfuel production. A substantial number of ethanol biorefineries operate in the area surrounding the nuclear plant selected for the case study analysis. Ethanol biorefineries emit a concentrated stream of CO_2 such that minimal additional processing steps are needed to obtain a high purity CO_2 feedstock for synfuel production. Additionally, since the CO_2 from the biorefineries is from a biogenic source, use of the synfuel produced using the biorefinery CO_2 source would result in low life-cycle carbon emissions.

The quantity of CO_2 feedstock required for synthetic fuel production depends on the capacity of the synfuel plant. For the scale of synfuel production operations examined in this analysis, the quantity of CO_2 feedstock required generally exceeds the amount that can be provided by a single biorefinery.

Therefore, CO_2 from several of the distributed ethanol biorefineries must be collected and transported to the centralized synfuel production plant in order to obtain the required quantity of CO_2 feedstock.

Larger capacity synfuel plants would require CO_2 feedstock from a larger number of distributed biorefineries. As the number of biorefineries needed to provide the required quantity of CO_2 feedstock increases, the average distance that the CO_2 must be transported increases. Longer CO_2 transport distances correspond to increased transport costs, so as the synfuel plant capacity increases, the average CO_2 feedstock cost should be expected to increase accordingly.

The following sections describe the methodology used to determine CO_2 feedstock costs and present a case study-specific CO_2 feedstock supply curve that estimates the CO_2 feedstock cost as a function of the quantity of CO_2 feedstock demanded. The CO_2 feedstock supply curve is subsequently used in the synfuel production economic analysis to evaluate the net present value (NPV) of synfuel production at various plant capacities, and to determine whether the economies of scale of synfuel production at large capacity outweigh the additional CO_2 feedstock costs associated with transporting the CO_2 feedstock long distances.

3.5.1 CO_2 Feedstock Supply Chain Overview

The CO_2 feedstock is assumed to be transported from the distributed biorefineries to the centralized synfuel production plant via pipeline. The following operations are considered in this CO_2 supply chain analysis: (1) CO_2 capture and compression to liquefy the gaseous CO_2; (2) storage in a temporary storage tank; and (3) transport through pipelines to the conversion site at the NPP. Figure 18 illustrates the sequence of the CO_2 supply chain operations.

Figure 18. CO_2 supply chain.

Based on the Braidwood NPP maximum power generation capacity of 2,386 MW-e, a maximum theoretical upper bound of CO_2 demand of 2.9 million metric tons per year was computed. The locations (latitude and longitude) of corn ethanol biorefinery plants and their yearly CO_2 production capacities were analyzed to produce a list of biorefineries located around the Braidwood plant that could provide up to the maximum quantity of CO_2 demand.

3.5.2 CO_2 Capture and Compression Cost

The gaseous CO_2 byproduct from corn ethanol biorefineries is saturated with water vapor and released from the plant at atmospheric pressure. The gaseous CO_2 must be compressed to a liquid-phase for cost-effective long-distance pipeline transportation. A pipeline inlet pressure of 150 bar (2176 psi) was specified for computing the compression power requirements. Analysis using Aspen Plus software indicates that the majority of the water vapor in the CO_2 byproduct can be removed upon compression with interstage cooling and knockout drums, resulting in a CO_2 stream with a purity of 99.8 mol% at 150 bar pressure. The compression energy requirements and compressor capital costs were computed based on the use of a nine-stage centrifugal compressor using methodology and calculations adapted from the "Current Central Hydrogen Production from Steam Methane Reforming of Natural Gas with CO_2 Capture and Sequestration" H2A case study [44].

Although in a deregulated market—such as the PJM market where the Braidwood plant operates—the nuclear-integrated synfuel plant would be able to obtain electrical power from the NPP at wholesale prices, the CO_2 transport pipeline network is expected to be operated by a separate corporate entity that would be required to purchase electrical power from the grid at retail prices. Average industrial sector retail electricity pricing data from form EIA-861 [45] was used to estimate the annual compressor and booster pump power costs; the East North Central region year 2020 average industrial sector electricity bill price of $67.8/MWhr from EIA-861 was used as the basis for calculating annual electric power costs for the CO_2 supply chain compressors and booster pumps.

3.5.3 Pipeline Transportation Cost

The National Energy Technology Laboratory (NETL) CO_2 Transport Cost Model [46] was used to compute the cost for transporting the liquid-phase CO_2 from ethanol plants to NPPs. The following assumptions were made in the CO_2 transport cost analysis:

1. The costs are computed for constructing new pipelines from ethanol plants to the NPP.

2. A separate pipeline is built to transport CO_2 from each neighboring ethanol plant to the NPP.

3. To compute the length of the pipeline between each distributed ethanol plant and the centralized NPP, it was assumed that CO_2 transport pipelines would follow a right-of-way that travels alongside existing roadways. An Open Street Routing Machine (OSRM) Application Programming Interface (API) in Python programming language was used to compute the road distance, which is the length of a given pipeline using the latitudes and longitudes of the ethanol plant and the NPP.

4. NETL CO_2 Transport Cost Model assumptions are followed for material, labor, operating, and maintenance costs related to pipeline construction.

5. A storage tank is considered in the supply side (i.e., near the ethanol plant location), which acts as a temporary storage in transporting the liquid CO_2 through the pipeline. Storage tank and pipeline control system costs of $701,600 and $94,000, respectively, are specified to be consistent with the NETL CO_2 Transport Cost Model. Based on data from Aspen Process Economic Analyzer, this corresponds to the cost of a vertical storage tank with a design pressure rating of 150 bar and a capacity of approximately 40 cubic meters, which provides storage capacity for approximately 33 metric tonnes of CO_2 (e.g., 825 kg/m³ density at 35°C and 150 bar).

The following inputs to the NETL CO_2 transport model were modified to calculate the transport costs for each pipeline segment between each ethanol biorefinery and the synfuel plant: (1) the length of the pipeline that was computed using the OSRM API; (2) the annual flow rate of CO_2 through the pipeline segment; (3) the region of the U.S. in which the pipeline is located; and (4) the per unit electricity cost (i.e., $/MWhr) in the region in which the pipeline is located. The NETL CO_2 Transport Cost Model was then used to compute the optimal pipeline diameter and the number of booster pumps along the pipeline length that minimize the cost of transporting CO_2 through each pipeline segment. The annualized CO_2 compression and transport costs for each pipeline segment were then used to construct the CO_2 feedstock supply curves.

3.5.4 Supply Curve

The CO_2 feedstock supply curve was computed by first identifying the set of the closest ethanol plants that have enough cumulative CO_2 production capacity to satisfy the upper bound of the CO_2 demand of that NPP. For example, as the upper bound of CO_2 demand of the Braidwood Nuclear Generating Station is 2.9 million metric tons per year (MMT/year), the nearest ethanol plants that have a combined CO_2 production capacity of at least 2.9 MMT/year were identified. The modified NETL CO_2 Transport Cost Model was then used to compute the cost of CO_2 logistics for each ethanol plant. By

24

sorting ethanol plant locations in increasing order of their CO_2 logistics costs, the cumulative average logistics costs were computed using Equation (5):

$$Cumulative\ average\ logistics\ cost = \frac{\sum_{i \in N} c_i q_i}{\sum_{i \in N} q_i} \qquad (5)$$

where:

- N is the set of ethanol plants considered in this computation indexed by i
- c_i is the cost of CO_2 logistics corresponding to the ethanol plant i
- q_i is the amount of CO_2 transported from ethanol plant i to the NPP.

The resulting supply curve illustrates the variation of this cumulative average cost of CO_2 logistics as a function of the total quantity of CO_2 transported to the synfuel plant. The CO_2 feedstock supply curve for the Braidwood NPP case study is shown in Figure 19.
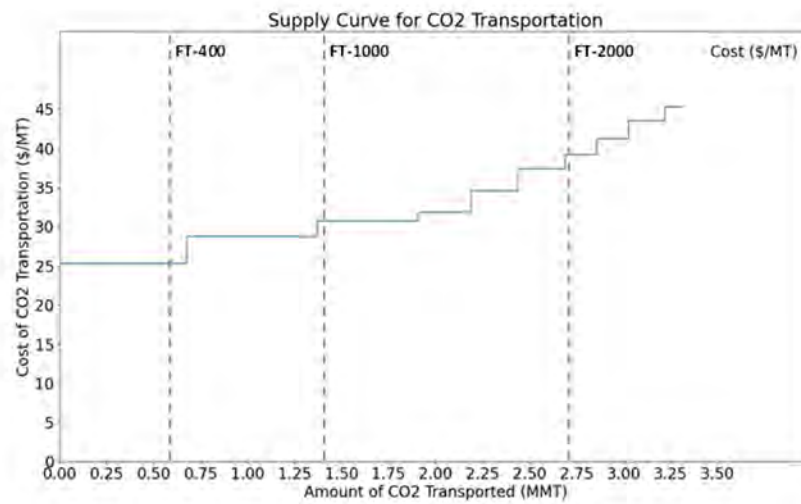

Figure 19. Supply curve for CO_2 transportation to Braidwood NPP.

3.6 Economic Analysis

3.6.1 Stochastic Techno-Economic Analysis via HERON

With RAVEN and its dispatch optimization plugin HERON, the computation of the NPV of the synthetic fuel production process is performed. The unpredictable behavior of electricity markets can be considered by using the signal processing and synthetic history capabilities of RAVEN. An ARMA model, discussed previously in Section 3.2.4, is used to analyze and reproduce price signals from the PJM market. Using this data, the optimal dispatch of the system's components is found and the NPV can then be computed.

3.6.2 Net Present Value Comparison Methodology

To assess the economic profitability of a system, its NPV can be computed—it requires the CAPEX and operation and maintenance (O&M) costs for all components. However, in the present analysis, the aim is to compare the economic benefit of using an NPP to make different products. Economic comparison of these different uses is the objective of this analysis. The differential NPV is the metric that is computed to determine which uses of the nuclear plant output would be most profitable. This approach eliminates the need for data regarding the costs of the NPP and the corresponding uncertainty, as shown in Equation (6).

$$\Delta NPV \ = \ NPV(System) - NPV(Baseline) \tag{6}$$

Equation (6) provides the calculation for this analysis, which is the NPV of the studied system that is compared to a "Baseline Case." The Baseline Case is chosen as the current use of the NPP (i.e., business-as-usual operating strategy in which all the power being produced is sold to the grid).

3.6.3   Synthetic Fuel Production Process HERON Model

As mentioned in the previous section, we compare the NPV of this system to the one of a Baseline Case. Figure 20 presents the Baseline Case: One 1193 MWe unit of the Braidwood NPP LWR sending all its electricity output to the PJM market. It allows us to compare the value of the current use of NPPs to shifting to a higher diversity of products and markets.
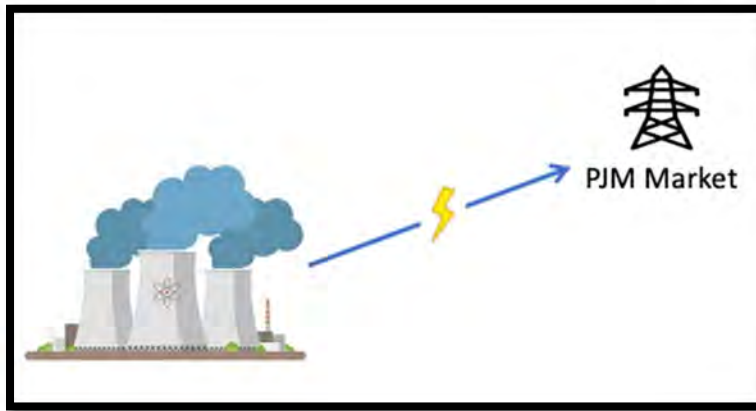
Figure 20. Baseline Case representing the current use of the NPP.

Figure 21 shows the synthetic fuels production process. The Braidwood NPP provides 1000 MW of power to a synfuel IES comprised of an electrolysis plant and an FT plant, and the balance of the power generation is sold to the grid (e.g., PJM market pricing data). The HTSE plant produces hydrogen for the FT process. CO_2 is also needed for this chemical process; it comes from nearby ethanol refineries. Three different synthetic fuel products are produced and sold: naphtha, diesel, and jet fuel. The annual production of each of these synfuel products is sold at the projected yearly price as detailed in Section 2. The project lifetime is 20 years, which corresponds to the license extension period the Braidwood NPP has recently been granted by the NRC. Table 7 shows the other financial assumptions made for this system and its analysis.

Figure 21 Synthetic fuel production process.

Table 7. Economic analysis financial assumptions.

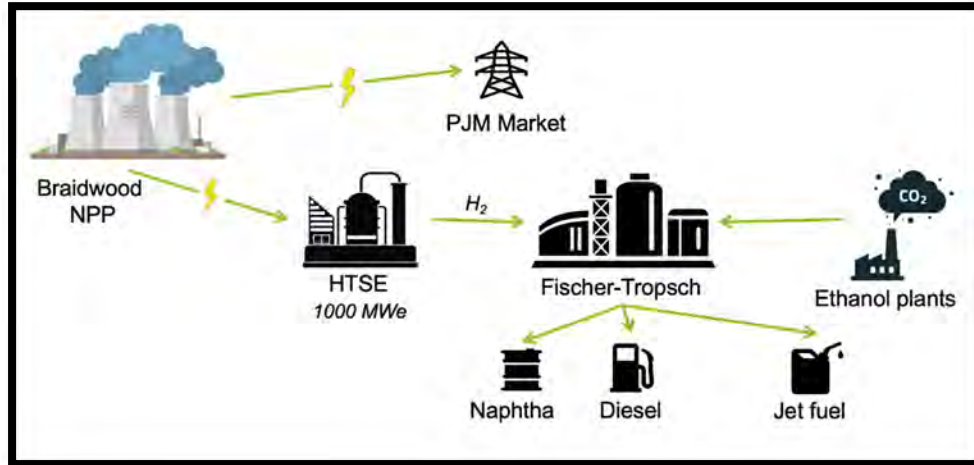| Parameter	Value	Description
Project life	20 years	Representative of the NRC NPP operating license extension period
Weighted Average Cost of Capital (WACC)	10%	
Inflation rate	2.18%	Average for 2000-2021
Federal corporate tax rate	21%	
Illinois corporate tax rate	9.50%	
Effective corporate tax rate	29.6%	
Depreciation schedule	15 years MACRS	
Synthetic fuel price	EIA AEO conventional fuels projection	See Section 2.4, Figure 3

Figure 22 presents the results of the NPV calculation for cases both with and without the Inflation Reduction Act of 2002 clean hydrogen production credits of $3/kg. Each case represents the differential NPV for production of synfuels relative to the Baseline Case of selling all power generated by the NPP to the electrical grid. A negative NPV therefore indicates that deployment of synfuel production IES would be less profitable than an NPP with dedicated electrical power sales, while a positive NPV indicates that a synfuel production IES would be more profitable than an NPP with dedicated electrical power sales. It should be noted that the differential NPV computes only the difference between the synfuel production case NPV and the Baseline Case NPV. Since the absolute NPV for the Baseline Case may not necessarily be positive, it is possible that even for a case in which the differential NPV is positive the synfuel production IES may not be economically viable.

Building an integrated energy system (IES) selling products on different markets results in a NPV decrease of $1.1 billion when no clean hydrogen PTCs are considered. Also shown in Figure 22 is the synthetic fuel production process Reference Case with the inclusion of the 2022 Inflation Reduction Act (IRA) clean hydrogen PTCs of $3/kg applied for the first ten years of plant operation. The 2022 IRA PTCs increase the NPV for the synfuel production process to $1.7 billion.
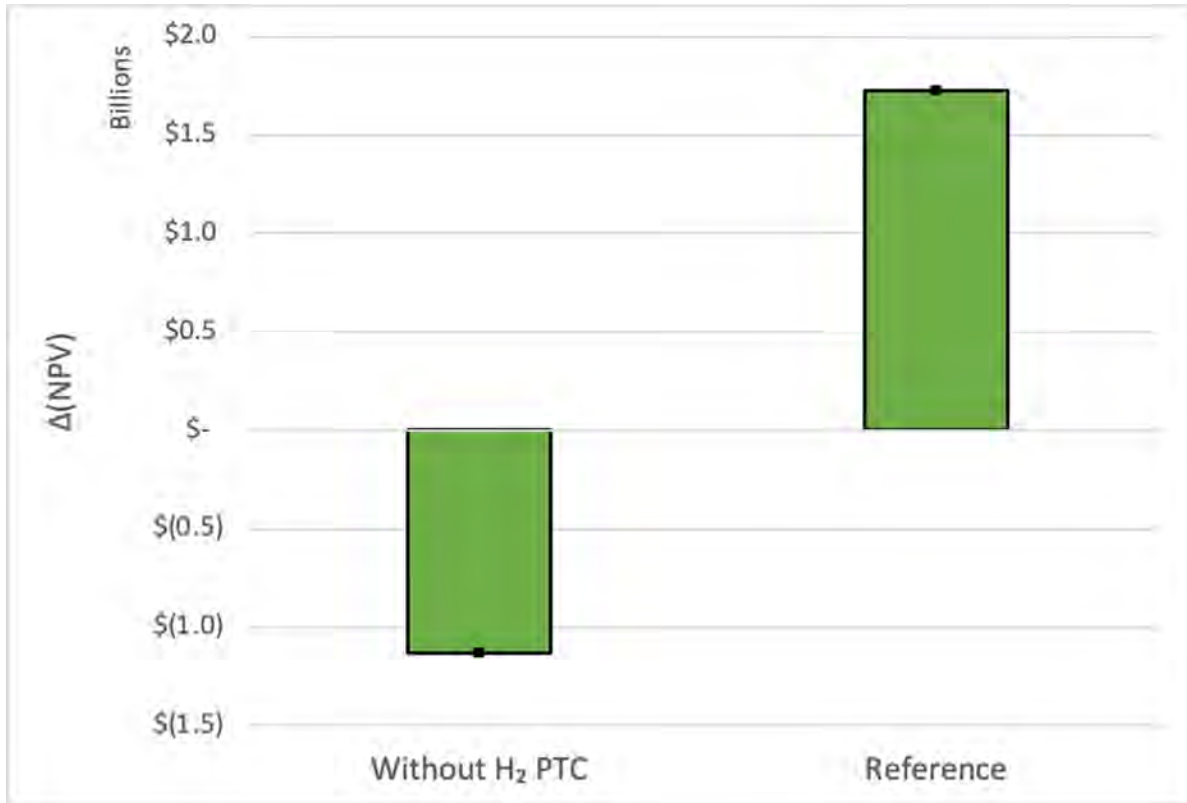
Figure 22. NPV comparison between the synfuels Reference Case with and without 2022 IRA clean hydrogen PTCs.

3.6.4 Sensitivity Analysis

Several assumptions were made in the design of the system analyzed in the previous section (the Reference Case)—the capacity of the HTSE plant was set to 1000 MWe, the prices for the synfuel products are set equal to conventional fuel products, and the NPP is assumed to be a price taker on the PJM market. To investigate the influence of these assumptions, a sensitivity analysis has been performed. The influence of the following variables has been compared:

- Electricity prices: Instead of a price taker assumption on the PJM market, the electricity price is set to the average price on either a regulated market (the High Electricity Price case) or a deregulated market (the Low Electricity Price case).

- Synthetic fuel products prices: Synthetic fuel products are lower in carbon than conventional fuel products and will thus benefit from various tax credits. To examine the influence of the prices of the products, the Reference Case was re-run with the original EIA conventional fuels projection adjusted downward by 20% (the Synfuel Low case) and upward by 20% (the Synfuel High case).

- Plant capacity: In the Reference Case the synfuel production capacity is 1000 MWe. The effect of synfuel plant capacity was examined by evaluating a case in with the synfuel production capacity was decreased to 400 MWe. This corresponds to more of the electricity generated by the NPP being sold to the grid instead of being used for synfuel production. The smaller synfuel plant has slightly higher capital costs (on a per production capacity unit basis) due to lower economies of scale, but also corresponds to lower CO_2 feedstock prices since the required feedstock quantity can be obtained from a smaller number of biorefineries (which has the effect of decreasing the average distance and cost of the CO_2 feedstock transport).

Figure 23 shows the results of the sensitivity analysis. We can observe that the capacity of the synfuel plant has the largest impact on the NPV of the system. A larger plant will indeed induce economies of scale. More importantly, it will generate more added value for the system via an increased amount of higher value synfuel products sold as compared to the Reference Case in which a higher proportion of the electricity produced by the nuclear reactor is directly sold to the grid. Synthetic fuel products prices are the next most influential variable, their production indeed represents a large added value for the system, and thus, modifying their prices will have a significant influence on the NPV of the system. Lastly, electricity prices have the least, but still a significant, influence on the economics of the system. As electricity brings less added value to the system, we could expect that the influence of electricity price would not be as large as that for the synthetic fuel products. The internal flows considered in the integrated system are not monetized: The cost of electricity used to produce hydrogen in the HTSE does not increase when electricity prices rise. The only costs of using electricity for synfuel production will stem from the O&M costs of the NPP and the synfuel plant. As a result, when electricity prices increase, the power produced by the NPP that is not used for hydrogen production is sold at a higher price on the electricity market, bringing additional revenue for the system.
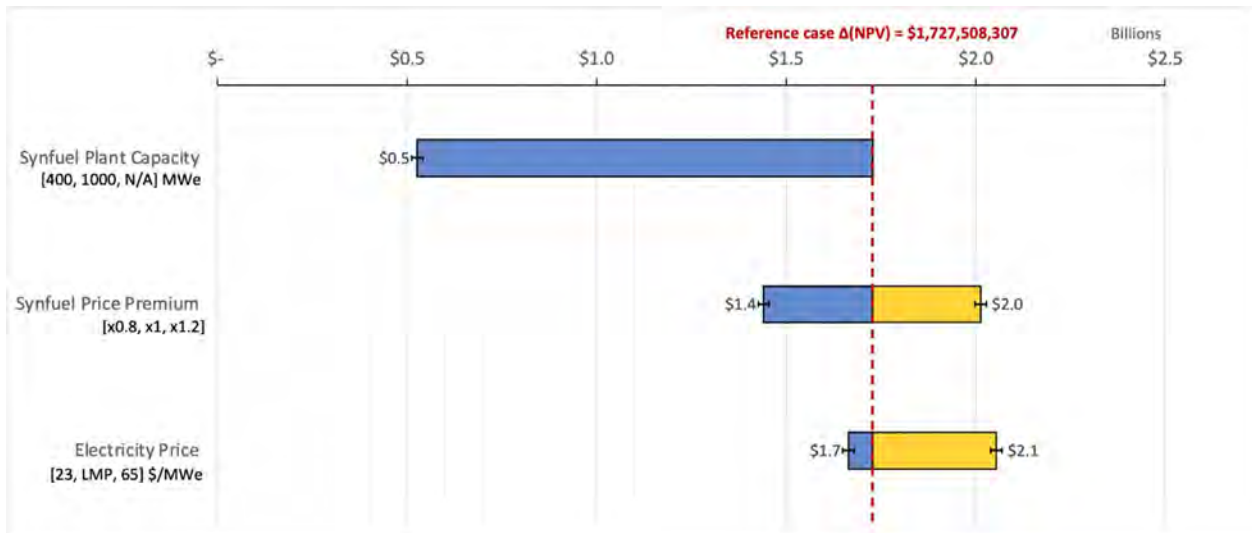

Figure 23. Synfuel production process sensitivity analysis results: influence of economies of scale, synfuel pricing, and electricity pricing.

4.   SUMMARY AND CONCLUSIONS

This economic analysis compared the NPV for the cases involving steady-state synfuel production with the NPV for a business-as-usual case in which the NPP continues to sell only electric power to the grid. A synfuel production Reference Case was considered in addition to sensitivity cases in which plant capacity, electricity price, and synthetic fuel product prices were perturbed. The synfuel production Reference Case considered a scenario in which the electrolysis and synfuel plants utilized a combined electrical load of 1000 MW-e from one unit of the NPP with the balance of the NPP power output being sold to the electric grid. Power sent to the grid is sold at prices based on historical 2018–2021 PJM LMP at the NPP node. Power diverted to the electrolysis and FT plants does not provide a direct source of revenue to the system; however, the synfuel products that are produced using this power provide a secondary revenue source to the system. Since the Synfuel IES includes the NPP, electrolysis plant, and FT plant, the flow of power from the NPP to the electrolysis and FT plants does not cross the system boundary, and therefore, is not monetized (i.e., the synfuel production cost does not depend on the electricity price, and the electricity price is applicable only for determining revenues from electric power sales to the grid). The Reference Case specified synthetic fuel pricing equal to that projected for conventional petroleum-based fuels in the U.S. EIA 2021 AEO minus federal taxes and state taxes, as well as marketing and distribution costs. The Reference Case incorporates the 2022 IRA clean hydrogen production credits of $3.00/kg into the revenue stream for the first ten years of operation.

The economic analysis suggests that the synfuel production Reference Case evaluated in this analysis would lead to considerable economic potential for near-term deployment of a nuclear-based synfuel production plant. Specifically, the economic analysis suggests that the deployment of a 1000 MW nuclear-powered synfuel plant could result in a NPV increase of approximately $1.7 billion for a case with no clean synfuel price premium relative to conventional petroleum fuels when accounting for the additional revenues from the 2022 IRA clean hydrogen PTCs of $3/kg.

The sensitivity analysis indicates that the plant capacity has the largest impact on the differential NPV with a smaller synfuel production capacity resulting in a decrease in revenues when a larger fraction of the power from the NPP is sold to the grid and a smaller fraction of the power is used to produce synthetic fuel products. The synfuel product pricing has the next largest impact on the differential NPV, with lower synfuel prices resulting in decreased NPV from decreased synfuel sales revenue while higher synfuel prices result in increased NPV from increased synfuel sales revenue. Electricity pricing has a smaller effect on the NPV than the fuel sales price since, in the Reference Case, most of the energy from the NPP is used for synfuel production and a smaller amount of the system revenues are associated with electrical power sales. However, the electricity price sensitivity does indicate that the Synfuel IES would have a greater NPV than the business-as-usual case for grid power sales only when electricity market prices are low, **suggesting that synfuel production could provide a strategy for decreasing the economic risks to NPPs posed by a loss of revenues attributed to falling electricity market prices.**

INL continues to evaluate nuclear-based synfuels production via the IES Program. Dynamic synfuel production operating schemes (i.e., feedstocks for synfuel production are produced during periods of low power pricing and electrical power is sent to the grid during peak periods), other CO_2 feedstock supply sources, and additional NPP case studies are being investigated in ongoing analyses.

5. REFERENCES

[1] U.S. Energy Information Administration (EIA), 2022, *Oil and Petroleum Products Explained: Use of Oil*, EIA, Washington D.C., USA. [online]. Available at: https://www.eia.gov/energyexplained/oil-and-petroleum-products/use-of-oil.php (last accessed 30 August 2022).

[2] U.S. Energy Information Administration (EIA), 2022, *Energy and the Environment Explained: Where Greenhouse Gases Come From*, EIA, Washington D.C, USA. [online]. Available at: https://www.eia.gov/energyexplained/energy-and-the-environment/where-greenhouse-gases-come-from.php (last accessed 30 August 2022).

[3] Shepardson, D., 2022, *Biden Renews Push for Sustainable Aviation Fuel Tax Credit*, Reuters, London, U.K. [online]. Available at: https://www.reuters.com/business/energy/biden-renews-push-sustainable-aviation-fuel-tax-credit-2022-04-12/ (last accessed 14 September 2022).

[4] Boeing, 2021, *Boeing Commits to Deliver Commercial Airplanes Ready to Fly on 100% Sustainable Fuels*, Boeing, Arlington, VA, USA. [online]. Available at: https://boeing.mediaroom.com/2021-01-22-Boeing-Commits-to-Deliver-Commercial-Airplanes-Ready-to-Fly-on-100-Sustainable-Fuels (last acessed 14 September 2022).

[5] Bioplastics Magazine, 2021, *Study Shows Renewable Naphtha Market Is Set For Robust Growth*, Bioplastics Magazine, Mönchengladbach, Germany. [online]. Available at: https://www.bioplasticsmagazine.com/en/news/meldungen/20211125-Study-shows-renewable-naphtha-market-is-set-for-robust-growth.php (last accessed 14 September 2022).

[6] Globe Newswire, 2022, *Global Diesel Market Size To Surpass US$ 1269.87 Billion By 2027 | Europe Having Share About 25% | Leading Players Strategies, Covid-19 Outbreak, Growth Opportunities, Emerging Trends, Segments Analysis, Business Outlook and Forecast 2027*, Globe Newswire, Los Angeles, CA, USA. [online]. Available at: https://www.globenewswire.com/en/news-release/2022/03/24/2409228/0/en/Global-Diesel-Market-Size-To-Surpass-US-1269-87-Billion-By-2027-Europe-Having-Share-About-25-Leading-Players-Strategies-Covid-19-Outbreak-Growth-Opportunities-Emerging-Trends-Segme.html (last accessed 14 September 2022).

[7] Lash, N., T. Melgin, A. Mucha-Geppert, and O. Rolser, 2022, *Charting the Global Energy Landscape to 2050: Sustainable Fuels*, McKinsey & Company, New York, NY, USA. [online]. Available at: https://www.mckinsey.com/industries/oil-and-gas/our-insights/charting-the-global-energy-landscape-to-2050-sustainable-fuels (last accessed 14 September 2022).

[8] U.S. Energy Information Administration (EIA), 2022, *Use of Energy Explained Energy Use for Transportation*, EIA, Washington D.C, USA. [online]. Available at: https://www.eia.gov/energyexplained/use-of-energy/transportation.php (last accessed 14 September 2022).

[9] Majewski, W. A., 2020, *Synthetic Diesel Fuel*, DieselNet, Mississauga, Ontario, Canada. [online]. Available at: https://dieselnet.com/tech/fuel_synthetic.php (last accessed 14 September 2022).

[10] Starn, J., 2021, *Shell Mulls Making Renewable Jet Fuel at New Swedish Facility*, Bloomberg, New York, NY, USA. [online]. Available at: https://www.bloomberg.com/news/articles/2021-11-03/shell-mulls-making-renewable-jet-fuel-near-swedish-nuclear-plant (last accessed 14 September 2022).

[11] Biofuels International, 2022, *Royal Air Force Marks New Stage in SAF Development*, Biofuels International, Morden, U.K. [online]. Available at: https://biofuels-news.com/news/royal-air-force-marks-new-stage-in-saf-development/ (last accessed 14 September 2022).

[12]   U.K. Ministry of Defence, 2022, *Sustainable Fuel Set to Power the Royal Air Force Reaches Landmark New Stage*, U.K. Ministry of Defence, London, U.K. [online]. Available at: https://www.gov.uk/government/news/sustainable-fuel-set-to-power-the-royal-air-force-reaches-landmark-new-stage#:~:text=The%20Royal%20Air%20Force%2C%20having,capability%20as%20a%20next%20stage (last accessed 14 September 2022).

[13]   U.S. Air Force, 2017, *Energy Flight Plan 2017–2036*, U.S. Air Force, Washington D.C., USA. [online]. Available at: https://www.afcec.af.mil/Portals/17/documents/Energy/AFEnergyFlightPlan2017.pdf?ver=2019-12-16-105948-090 (last accessed 14 September 2022).

[14]   Poland, C., 2021, *The Air Force Partners with Twelve, Proves It's Possible to Make Jet Fuel Out of Thin Air*, U.S. Air Force, Arlington, VA, USA. [online]. Available at: https://www.af.mil/News/Article-Display/Article/2819999/the-air-force-partners-with-twelve-proves-its-possible-to-make-jet-fuel-out-of/ (last accessed 14 September 2022).

[15]   United Airlines (UAL), 2021, *United, Honeywell Invest in New Clean Tech Venture from Alder Fuels, Powering Biggest Sustainable Fuel Agreement in Aviation History*, UAL, Chicago, IL, USA. [online]. Available at: https://www.united.com/en/us/newsroom/announcements/united-honeywell-invest-in-new-clean-tech-venture-from-alder-fuels-powering-biggest-sustainable-fuel-agreement-in-aviation-history-2654951909 (last accessed 14 September 2022).

[16]   U.S. Department of Energy–Office of Energy Efficiency and Renewable Energy (DOE-EERE), 2020, *Sustainable Aviation Fuel: Review of Technical Pathways*, DOE/EE-2041, DOE-EERE, Washington D.C., USA. [online]. Available at: https://www.energy.gov/sites/prod/files/2020/09/f78/beto-sust-aviation-fuel-sep-2020.pdf (last accessed 14 September 2022).

[17]   Daily Sabah, 2022, *Sanctions on Russia May Trigger Global Diesel Supply Crisis*, Daily Sabah, Istanbul, Turkey. [online]. Available at: https://www.dailysabah.com/business/energy/sanctions-on-russia-may-trigger-global-diesel-supply-crisis (last accessed 14 September 2022).

[18]   U.S. Energy Information Administration (EIA), 2022, *Energy Information Administration, Refinery Capacity 2022*, EIA, Washington, D.C., USA. [online]. Available at: https://www.eia.gov/petroleum/refinerycapacity/ (last accessed 14 September 2022).

[19]   U.S. Department of Energy–Office of Energy Efficiency and Renewable Energy (DOE-EERE), n.d., *Sustainable Aviation Fuel Grand Challenge*, DOE-EERE, Bioenergy Technologies Office, Washington D.C., USA. [online]. Available at: https://www.energy.gov/eere/bioenergy/sustainable-aviation-fuel-grand-challenge (last accessed 14 September 2022).

[20]   Guarascio, F., 2022, *EU Lawmakers Back Mandatory Use of Green Jet Fuel from 2025*, Reuters, London, U.K. [online]. Available at: https://www.reuters.com/business/aerospace-defense/eu-lawmakers-back-mandatory-use-green-jet-fuel-2025-2022-07-07/ (last accessed 14 September 2022).

[21]   World Economic Forum (WEF), 2021, *Guidelines for a Sustainable Aviation Fuel Blending Mandate in Europe: Insight Report*, July 2021, WEF, Geneva, Switzerland. [online]. Available at: https://www3.weforum.org/docs/WEF_CST_EU_Policy_2021.pdf (last accessed 14 September 2022).

[22]   World Economic Forum (WEF), 2021, *What 6 Aviation Executives Say About an EU Sustainable Aviation Fuel Blending Mandate*, WEF, Geneva, Switzerland. [online]. Available at: https://www.weforum.org/agenda/2021/07/what-6-executives-europe-aviation-sector-say-eu-sustainable-fuel-saf-blending-mandate-refueleu/ (last accessed 14 September 2022).

[23]   Bousso, R., 2021, *Oil Giant Shell Sets Sights on Sustainable Aviation Fuel Take-Off*, Rueters, London, U.K. [online]. Available at: https://www.reuters.com/business/sustainable-business/oil-giant-shell-sets-sights-sustainable-aviation-fuel-take-off-2021-09-19/ (last accessed 14 September 2022).

[24] Li, X., P. Anderson, H.-R. M. Jhong, M. Paster, J. F. Stubbins, and P. J. A. Kenis, 2016, "Greenhouse gas emissions, energy efficiency, and cost of synthetic fuel production using electrochemical CO_2 conversion and the Fischer–Tropsch process," *Energy & Fuels,* vol. 30, no. 7, pp. 5980–5989. https://doi.org/10.1021/acs.energyfuels.6b00665.

[25] U.S. Energy Information Administration (EIA), 2022, *Annual Energy Outlook 2022*, EIA, Washington D.C, USA. [online]. Available at: https://www.eia.gov/outlooks/aeo/ (last accessed 14 September 2022).

[26] U.S. Energy Information Administration (EIA), 2022, *Gasoline Explained: Factors Affecting Gasoline Prices*, EIA, Washington D.C, USA. [online]. Available at: https://www.eia.gov/energyexplained/gasoline/factors-affecting-gasoline-prices.php (last accessed 14 September 2022).

[27] Trading Economics, 2022, *Naphtha*, Trading Economics, New York NY, USA. [online]. Available at: https://tradingeconomics.com/commodity/naphtha (last accessed 14 September 2022).

[28] Constellation Energy, 2022, *Braidwood Generating Station*, Constellation Energy, Baltimre, MD, USA. [online]. Available at: https://www.constellationenergy.com/our-company/locations/location-sites/braidwood-generating-station.html (last accessed 14 September 2022).

[29] National Renewable Energy Laboratory, 2022, *Biofuels Atlas*, National Renewable Energy Laboratory, Golden, CO, USA. [online]. Available at: https://maps.nrel.gov/biofuels-atlas (last accessed 14 September 2022).

[30] Customer First Renewables, n.d., *Regulated & Deregulated Energy Markets*, Customer First Renewables, Gaithersburg, MD, USA. [online]. Available at: https://infocastinc.com/market-insights/solar/regulated-deregulated-energy-markets/ (last accessed 14 September 2022).

[31] Frick, K., P. Talbot, D. Wendt, R. Boardman, C. Rabiti, S. Bragg-Sitton, D. Levie, B. Frew, M. Ruth, A. Elgowainy, and T. Hawkins, 2019, *Evaluation of Hydrogen Production Feasibility for a Light Water Reactor in the Midwest*, INL/EXT-19-55395, September 2019, Idaho National Laboratory, Idaho Falls, ID, USA. https://doi.org/10.2172/1569271.

[32] Chen, J., and C. Rabiti, 2017, "Synthetic wind speed scenarios generation for probabilistic analysis of hybrid energy systems," *Energy,* vol. 120, pp. 507–517. https://doi.org/10.1016/j.energy.2016.11.103.

[33] Talbot, P. W., C. Rabiti, A. Alfonsi, C. Krome, M. R. Kunz, A. Epiney, C. Wang, and D. Mandelli, 2020, "Correlated synthetic time series generation for energy system simulations using Fourier and ARMA signal processing," *International Journal of Energy Research,* vol. 44, no. 10, pp. 8144–8155. https://doi.org/10.1002/er.5115.

[34] Delgado, H. E., V. Cappello, P. Sun, C. Ng, P. Vyawahare, and A. Elgowainy, 2022, *The Modeling of the Synfuel Production Process: Techno-Economic Analysis and Life Cycle Assessment of FT Fuel Production Plants Integrated with Nuclear Power*, ANL/ESD-22/41, June 2022, Argonne National Laboratory, Argonne, IL, USA.

[35] Zang, G., P. Sun, and A. Elgowainy, 2021, *The Modeling of Synfuel Production Process: ASPEN Model of FT Production With Electricity Demand Provided at LWR Scale*, ANL/ESD-22/1, December 2021, Argonne National Laboratory, Argonne, IL, USA. [online]. Available at: https://publications.anl.gov/anlpubs/2022/02/173337.pdf (last accessed 26 September 2022).

[36] Zang, G., P. Sun, H. E. Delgado, V. Cappello, C. Ng, and A. Elgowainy, 2022, *The Modeling of the Synfuel Production Process: Process Models of Fischer-Tropsch Production with Electricity and Hydrogen Provided by Various Scales of Nuclear Plants*, ANL/ESD-22/8, April 2022, Argonne National Laboratory, Argonne, IL, USA. [online]. Available at: https://publications.anl.gov/anlpubs/2022/05/175009.pdf (last accessed 26 September 2022).

[37] Laguna-Bercero, M. A., 2012, "Recent advances in high temperature electrolysis using solid oxide fuel cells: A review," *Journal of Power Sources,* vol. 203, pp. 4–16. https://doi.org/10.1016/j.jpowsour.2011.12.019.

[38]   Schmidt, O., A. Gambhir, I. Staffell, A. Hawkes, J. Nelson, and S. Few, 2017, "Future cost and performance of water electrolysis: An expert elicitation study," *International Journal of Hydrogen Energy,* vol. 42, no. 52, pp. 30470–30492. https://doi.org/10.1016/j.ijhydene.2017.10.045.

[39]   Wendt, D. S., L. T. Knighton, and R. D. Boardman, 2022, *High-Temperature Steam Electrolysis Process Performance and Cost Estimates*, INL/RPT-22-66117, March 2022, Idaho National Laboratory, Idaho Falls, ID, USA. [online]. Available at: https://inldigitallibrary.inl.gov/sites/sti/sti/Sort_60759.pdf.

[40]   James, B. D., and B. Murphy, 2021, "Solid Oxide Electrolysis Stack Manufacturing Cost Analysis," April 2021, Strategic Analysis, Inc., Arlington, VA, USA.

[41]   Frøhlke, U., 2022, *Topsoe Confirms Final Investment Decision for Construction of World's Largest SOEC Electrolyzer Plant*, Topsoe, Lyngby, Denmark. [online]. Available at: https://blog.topsoe.com/topsoe-confirms-final-investment-decision-for-construction-of-worlds-largest-electrolyzer-plant (last accessed 26 September 2022).

[42]   O'Brien, J. E., J. L. Hartvigsen, R. D. Boardman, J. J. Hartvigsen, D. Larsen, and S. Elangovan, 2020, "A 25 kW high temperature electrolysis facility for flexible hydrogen production and system integration studies," *International Journal of Hydrogen Energy,* vol. 45, no. 32, pp. 15796–15804. https://doi.org/10.1016/j.ijhydene.2020.04.074.

[43]   Peterson, D., J. Vickers, and D. DeSantis, 2020, *DOE Hydrogen and Fuel Cells Program Record #20006: Hydrogen Production Cost from High Temperature Electrolysis - 2020*, U.S. Department of Energy Hydrogen and Fuel Cell Technologies Office, Washington, D.C., USA. [online]. Available at: https://www.hydrogen.energy.gov/pdfs/20006-production-cost-high-temperature-electrolysis.pdf (last accessed 26 September 2022).

[44]   U.S. Department of Energy (DOE) Hydrogen and Fuel Cells Technologies Office, 2018, *Hydrogen Analysis (H2A) Production Model*, DOE Hydrogen and Fuel Cells Technologies Office, Washington, D.C., USA. [online]. Available at: https://www.hydrogen.energy.gov/h2a_production.html (last accessed 26 September 2022).

[45]   U.S. Energy Information Administration (EIA), 2021, *Electric Sales, Revenue, and Average Price*, EIA, Washington D.C, USA. [online]. Available at: https://www.eia.gov/electricity/sales_revenue_price/ (last accessed 26 September 2022).

[46]   Morgan, D., T. Grant, and D. Remson, "FECM/NETL CO_2 Transport Cost Model (2022)," DOE/NETL-2022/3243, March 14 2022, National Energy Technology Laboratory, Pittsburgh, PA, USA. [online]. Available at: https://netl.doe.gov/projects/VueConnection/download.aspx?id=046f9b76-123d-456b-b29e-57e027a099df&filename=FECMNETLCO2TransportCostModel2022_031422.xlsm (last accessed 26 September 2022).

[47]   Bandara, K., R. J. Hyndman, and C. Bergmeir, 2021, "MSTL: A seasonal-trend decomposition algorithm for time series with multiple seasonal patterns," 29 July 2021. [online]. Available at: https://arxiv.org/abs/2107.13462 (last accessed 26 September 2022).

Appendix A –
2018–2021 PJM Market LMP Data Analysis

Appendix A –
2018–2021 PJM Market LMP Data Analysis

In order to better understand the trend and seasonal distribution of the RT-LMP in 2018 and 2019, we employed the Multiple Seasonal-Trend decomposition using Loess (MSTL) algorithm, which is a fully automated, additive time series decomposition algorithm to handle time series with multiple seasonal cycles to analyze the RT-LMP data obtained during 2018 and 2019. This most recently proposed MSTL algorithm [47] is an extended version of the STL decomposition algorithm, where the STL procedure is applied iteratively to estimate the multiple seasonal components in a time series. This allows MSTL to control the smoothness of the change of seasonal components for each seasonal cycle extracted from the time series, and seamlessly separate their seasonal variations (e.g., deterministic, stochastic seasonality). In particular, we decompose the hourly time series of RT-LMP in a year, Xt into trend Tt, daily seasonal component StD, weekly seasonal component StW, and the remainder Rt, as shown in Equation (7).

$$X_t = T_t + S_{tD} + S_{tW} + R_t, \quad t=1,2,\ldots,8760 \tag{7}$$

Figure 24 and Figure 26 show the trends of the RT-LMP evolution in 2018 and 2019, respectively. The snapshot of daily seasonal and weekly seasonal decomposition components showing in Figure 25 and Figure 27 indicate that the daily seasonality and weekly seasonality of RT-LMP have been well captured by this MSTL decomposition algorithm. In particular, in Figure 25(a), we have identified at least one peak price in the afternoon within a single day in January, June, and September 2018. In January 2018, another daily peak price takes place in the early morning, which corresponds to the high electricity demand for housewarming during the coldest time of the winter. Similar phenomena can be observed in the other years (2019, 2020 and 2021). Due to the same reason associated with weather, as for the weekly seasonality shown in Figure 25(b), we find higher and increasing RT-LMP on the weekends in January 2018. In June and September, a lower and decreasing RT-LMP is observed on the weekends due to the increase in outdoor activities in summer and fall. Similar conclusions can be obtained from Figure 27 for 2019 as well. During the pandemic, the lowest electricity price in 2020 has been identified in April (see Figure 28 for trend), which is associated with the lockdown policy at the beginning of the pandemic. As for the daily and weekly seasonality, it does not show a significant difference comparing the years before the pandemic and after the pandemic.

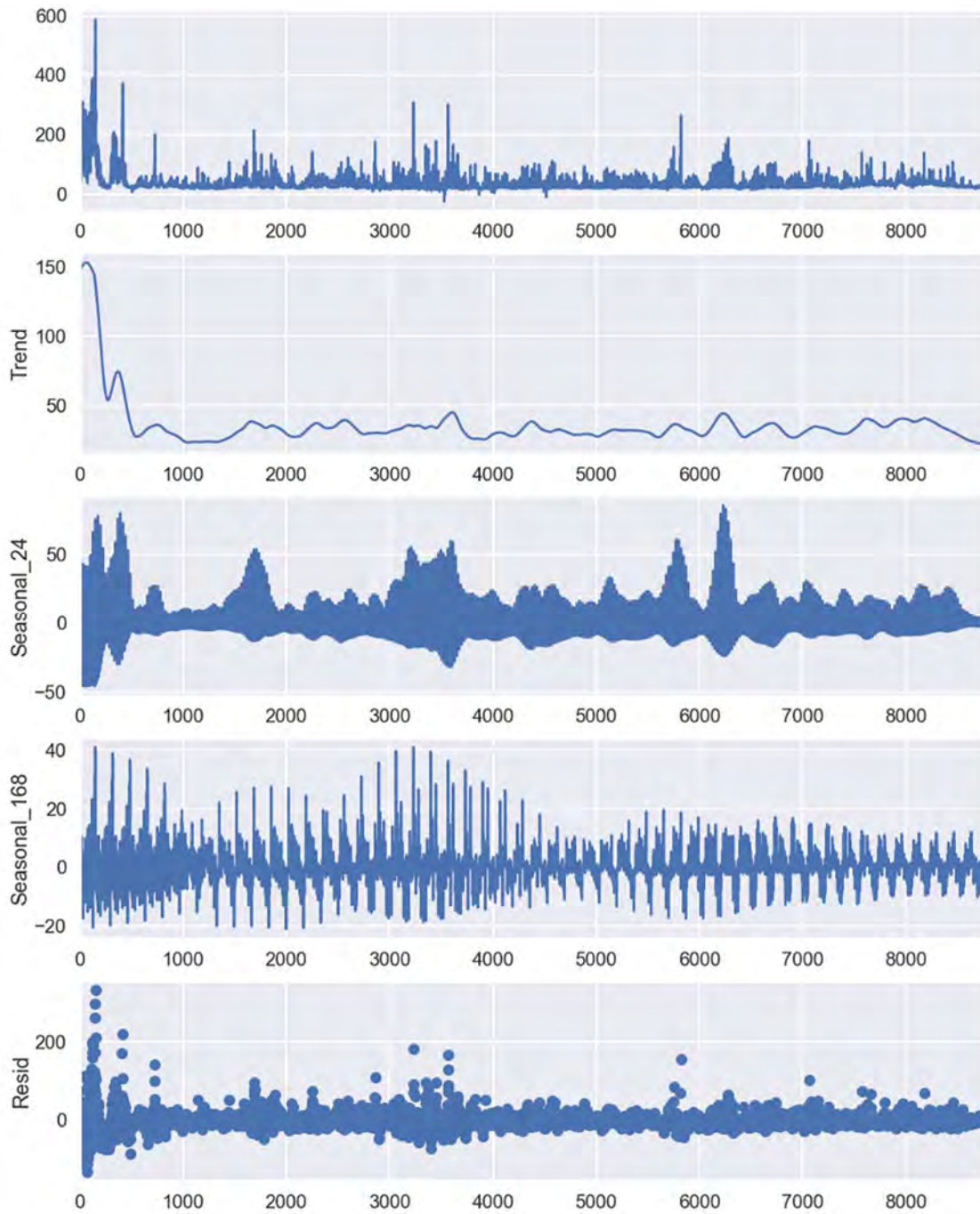**Multi-seasonal time series decomposition for RT-LMP in 2018**

Figure 24. The decomposition of hourly RT-LMP at Braidwood NPP in 2018 using MSTL. Each panel represents the original data, the trend, the daily seasonality, the weekly seasonality, and the remainder, respectively.
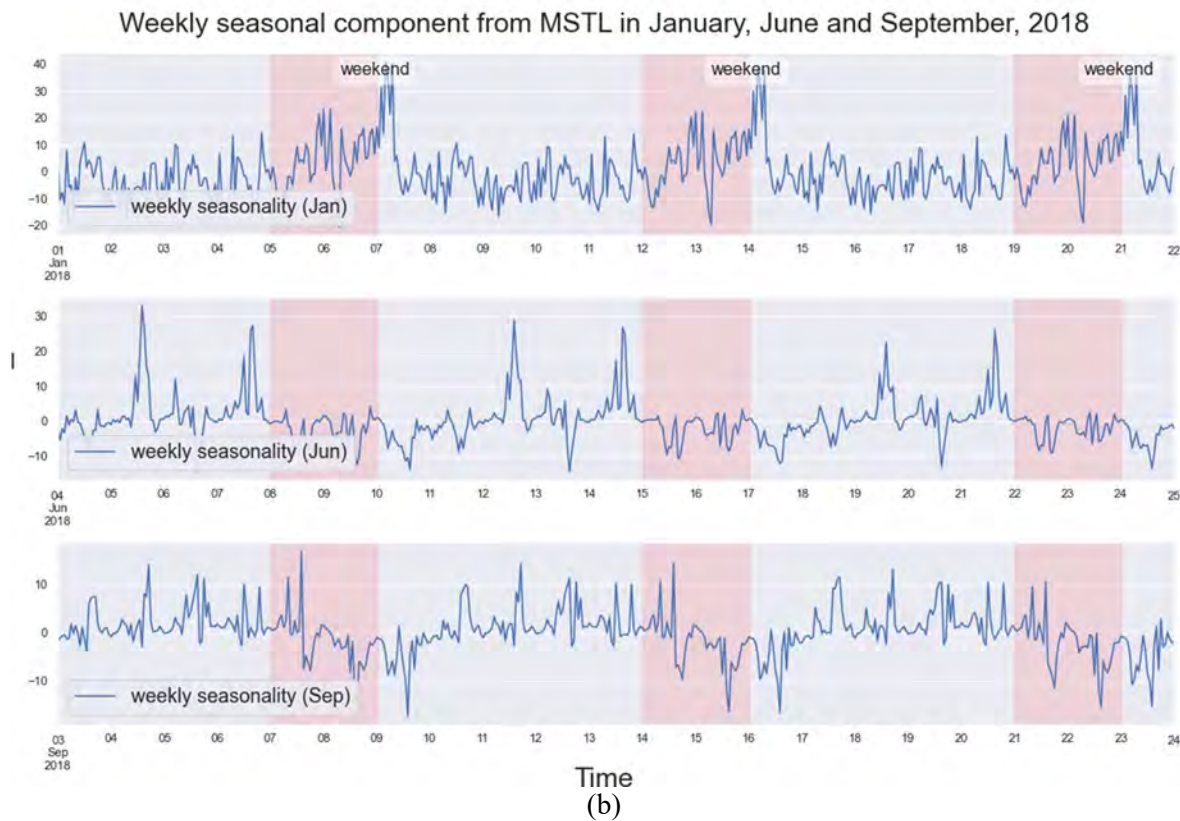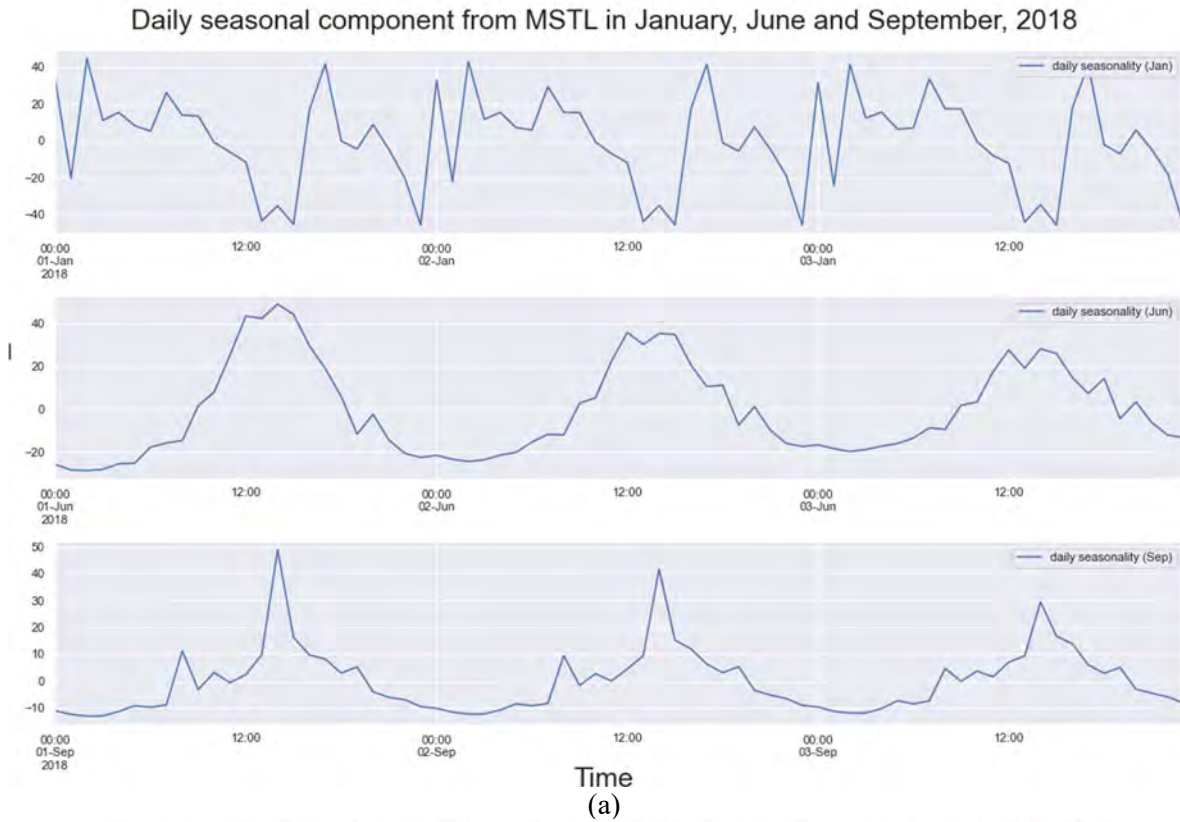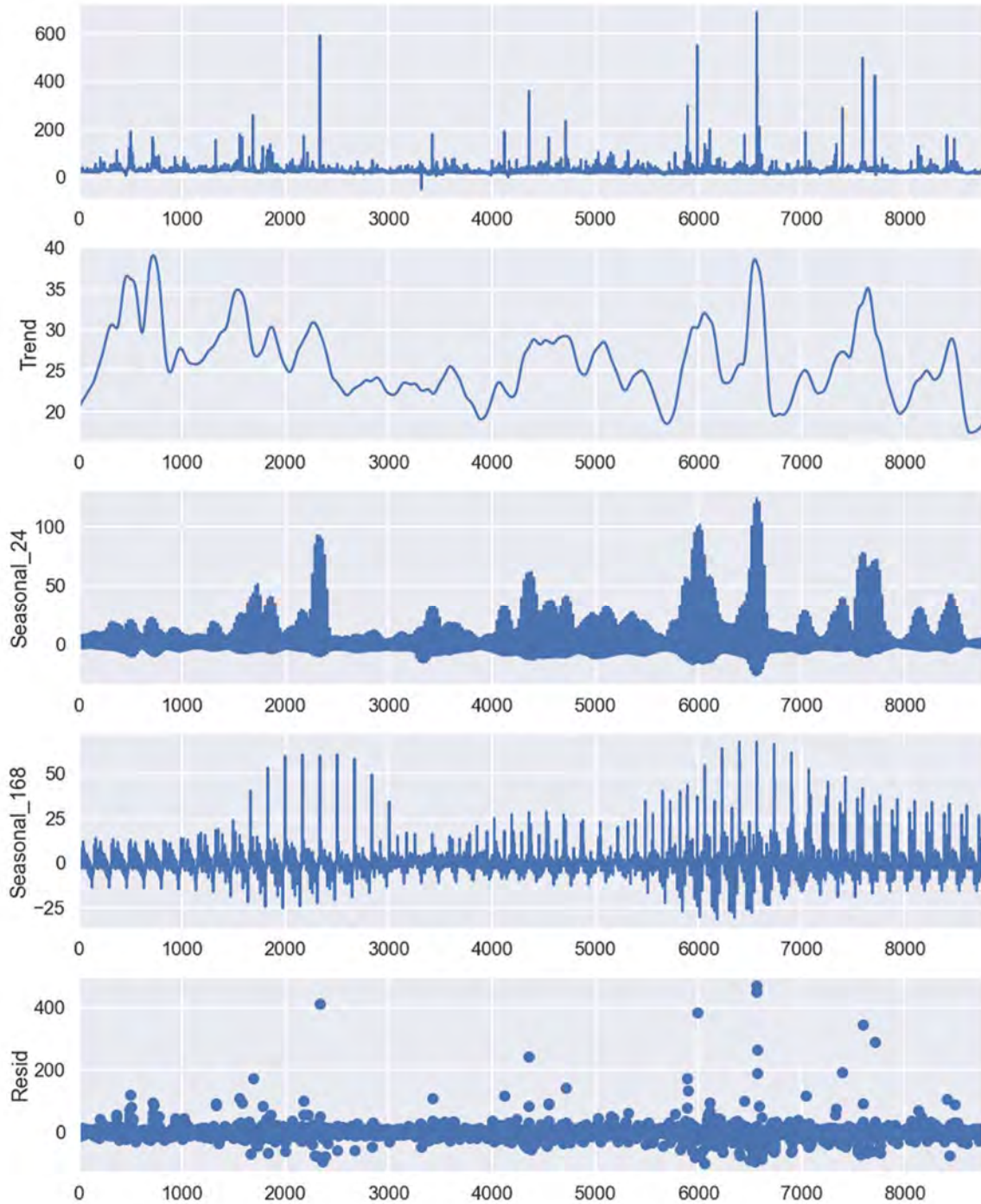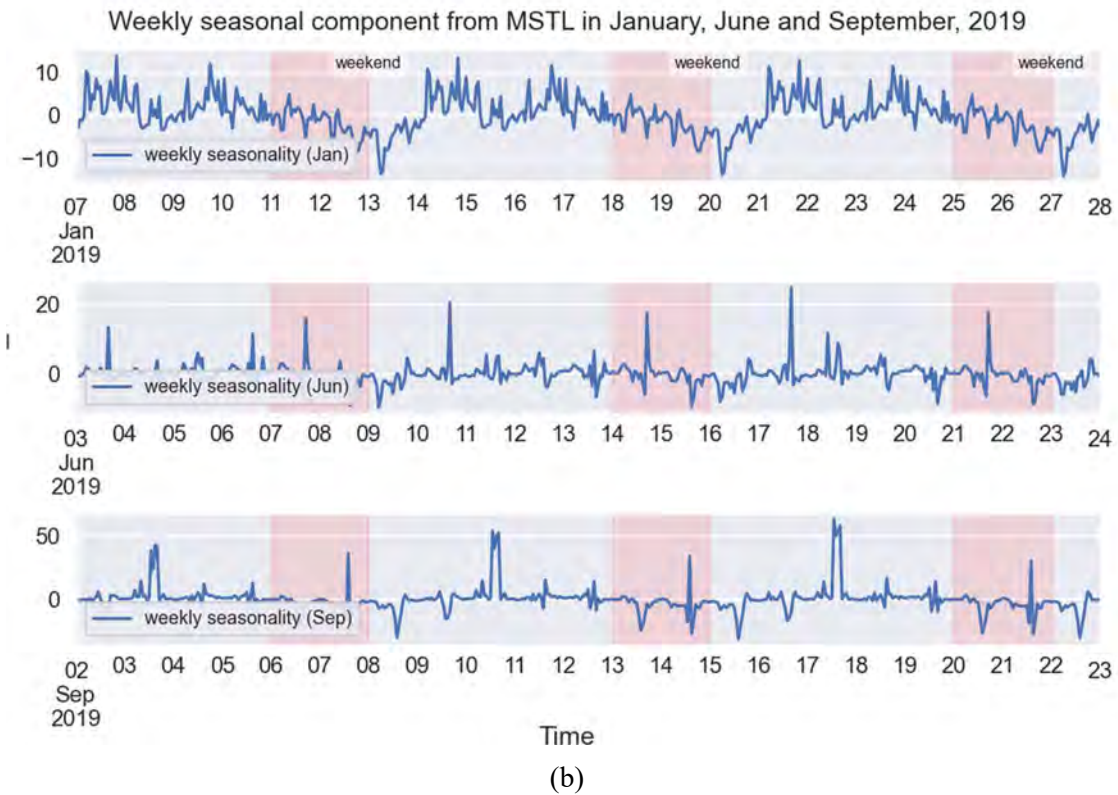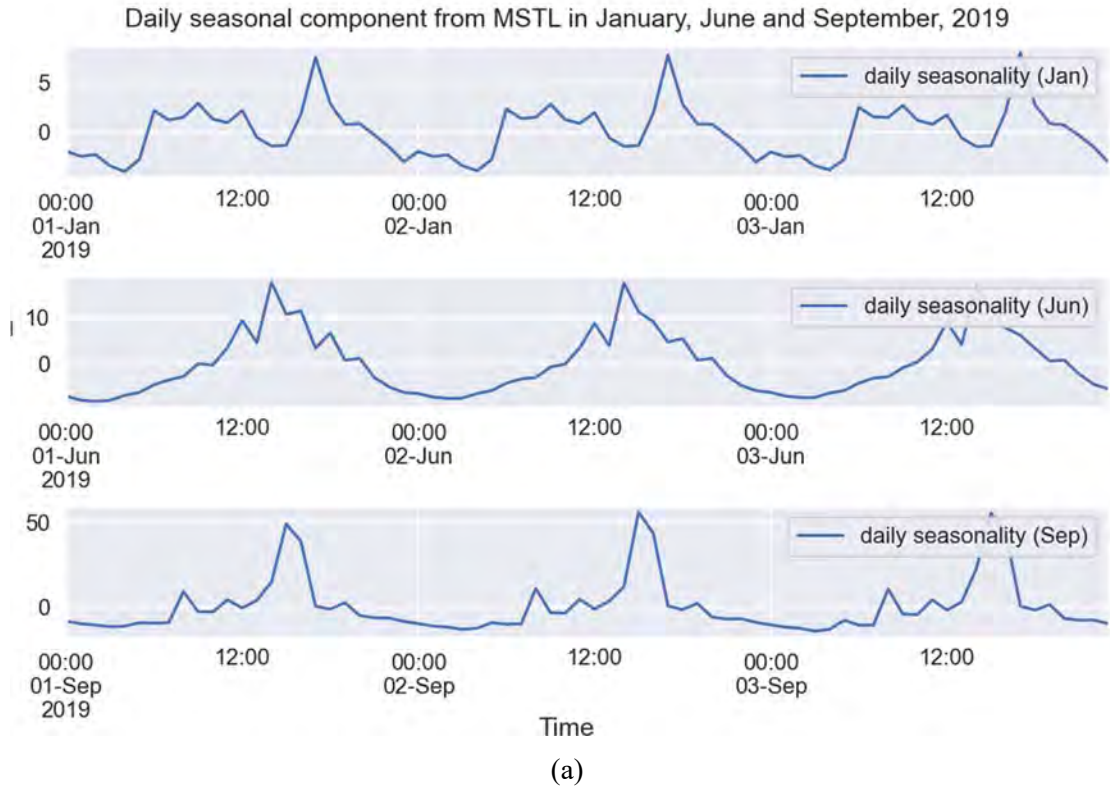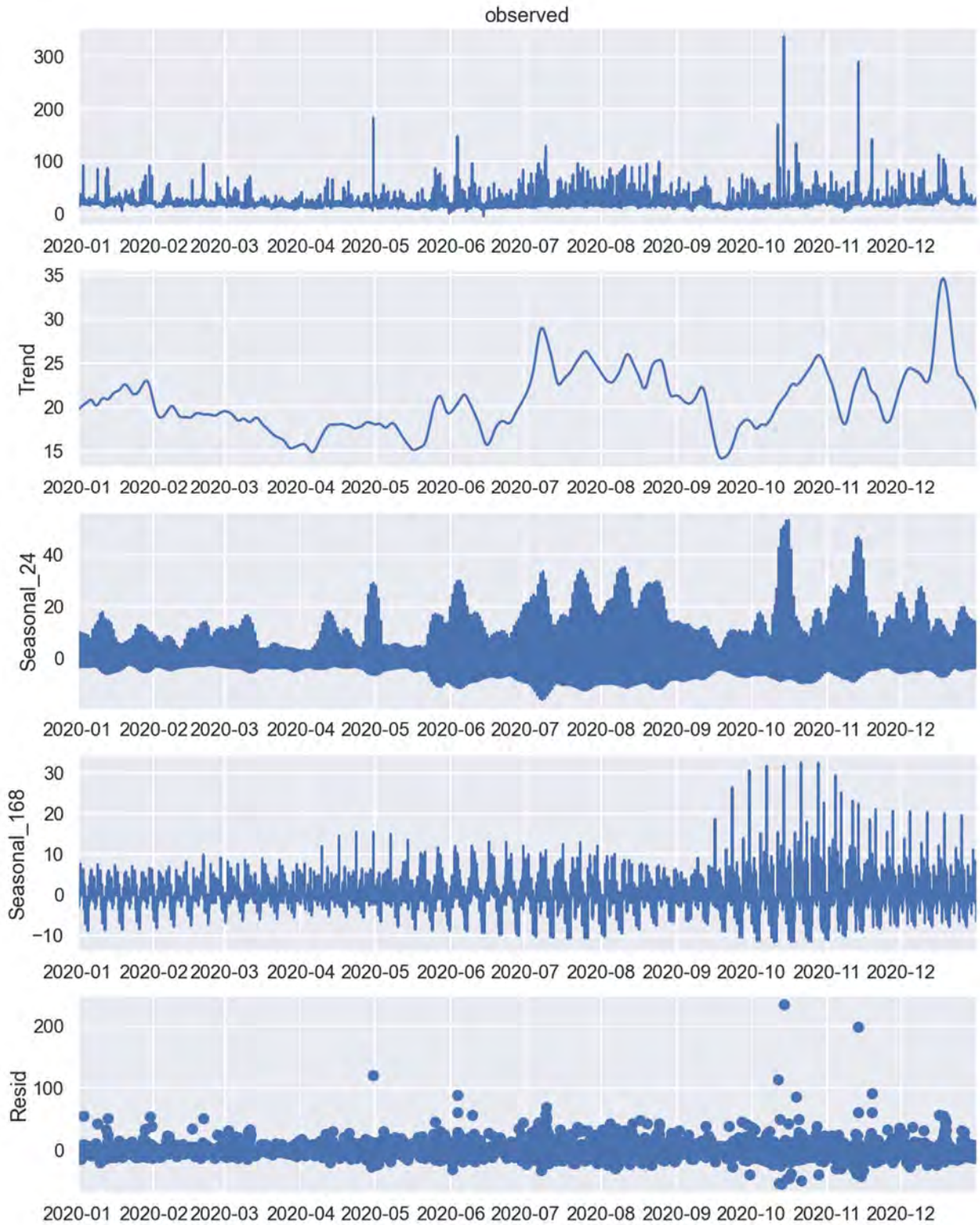
Figure 25. (a) Three-day snapshot of the daily seasonal component in January, June, and September 2018. (b) Three-week snapshot of the weekly seasonal component in January, June, and September 2018.

Multi-seasonal time series decomposition for RT-LMP in 2019

Figure 26. The decomposition of hourly RT-LMP at Braidwood NPP in 2019 using MSTL. Each panel represents the original data, the trend, the daily seasonality, the weekly seasonality, and the remainder, respectively.
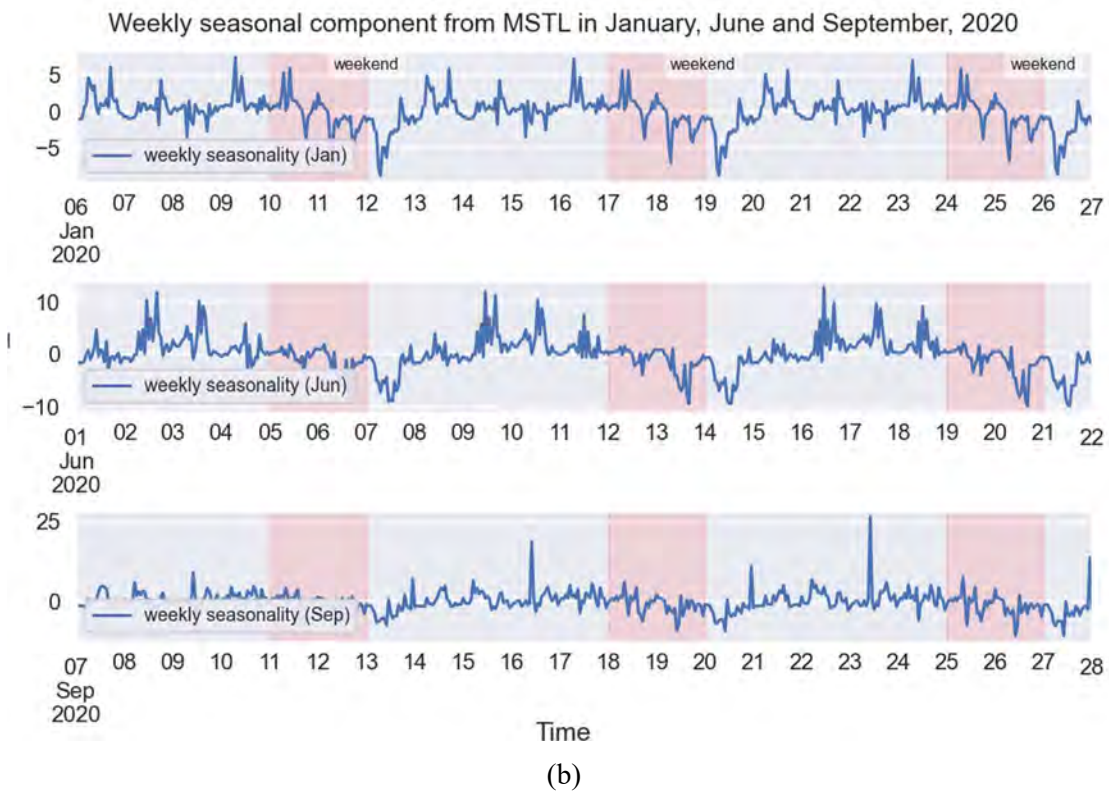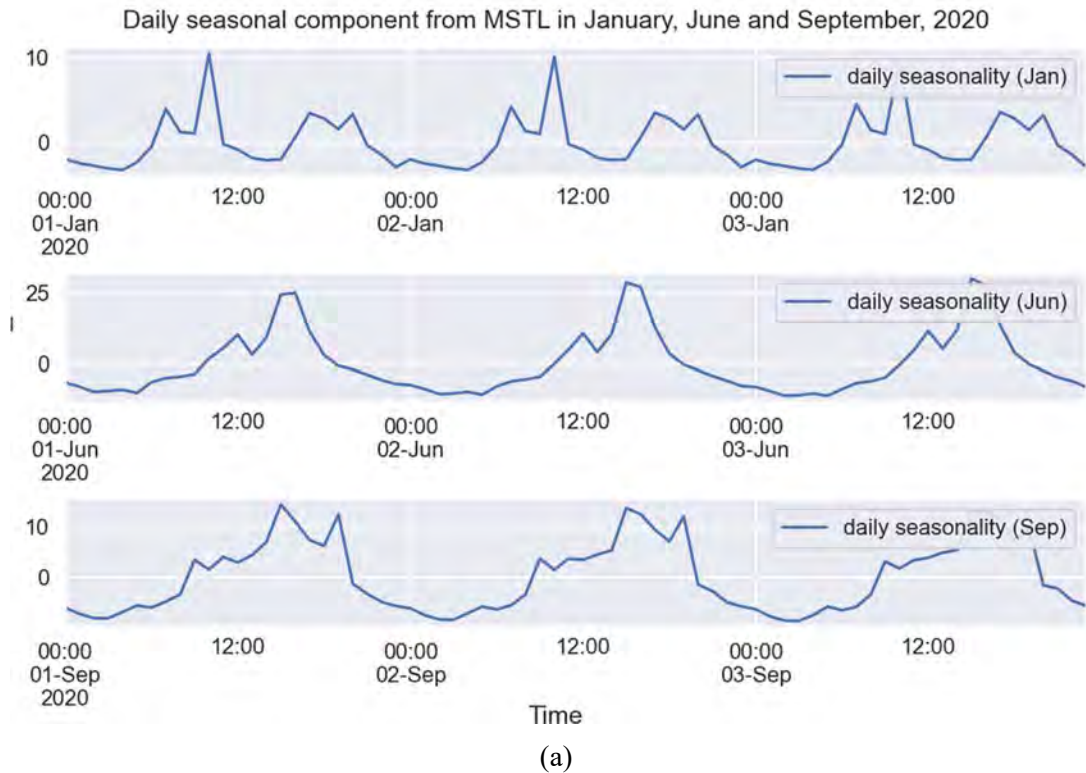
Figure 27. (a) Three-day snapshot of the daily seasonal component in January, June, and September 2019. (b) Three-week snapshot of the weekly seasonal component in January, June, and September 2019.

Multi-seasonal time series decomposition for RT-LMP in 2020

Figure 28. The decomposition of hourly RT-LMP at Braidwood NPP in 2020 using MSTL Each panel represents the original data, the trend, the daily seasonality, the weekly seasonality, and the remainder respectively.

Figure 29. (a) Three-day snapshot of the daily seasonal component in January, June, and September 2020. (b) Three-week snapshot of the weekly seasonal component in January, June, and September 2020.

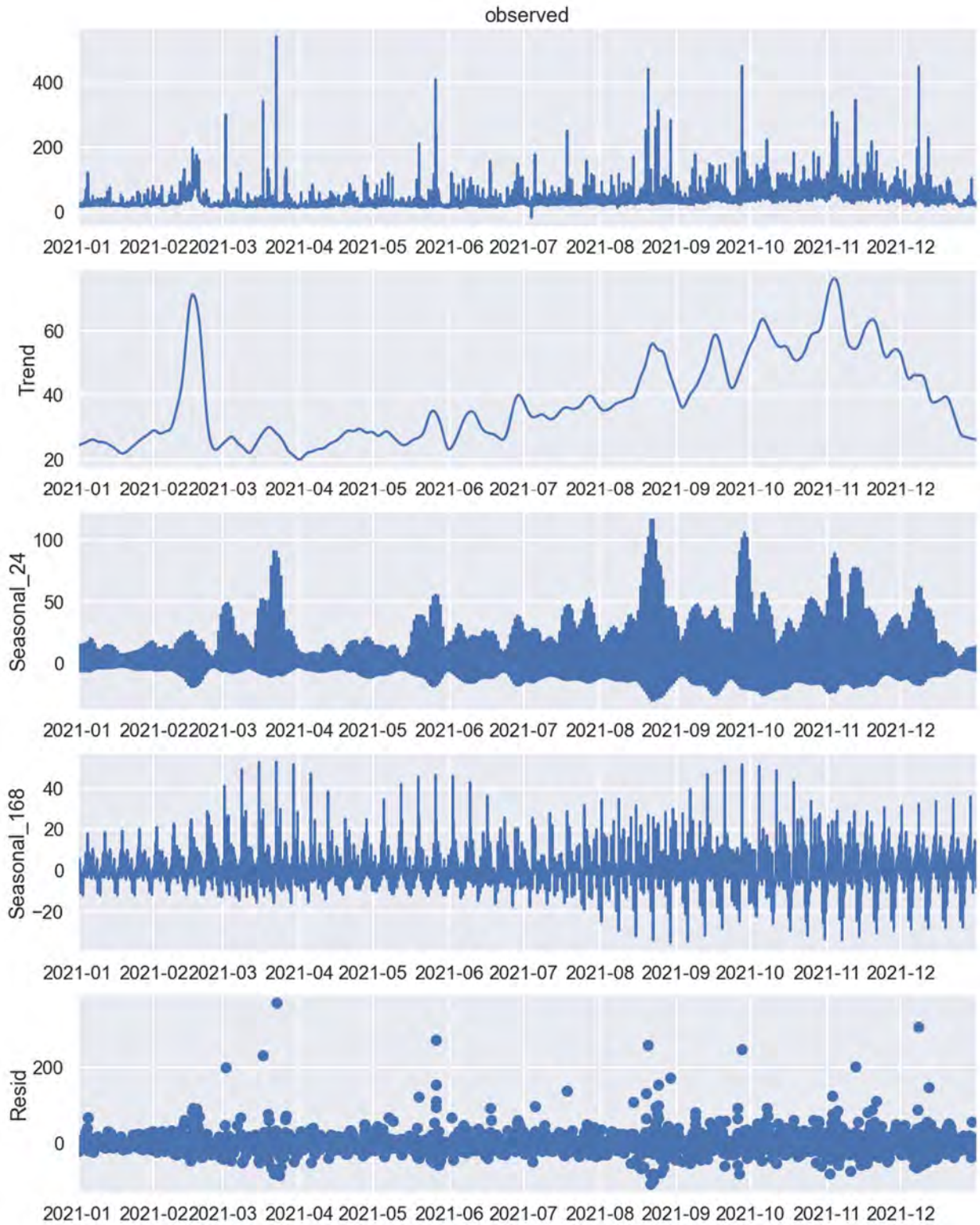**Multi-seasonal time series decomposition for RT-LMP in 2021**

Figure 30. The decomposition of hourly RT-LMP at Braidwood NPP in 2021 using MSTL. Each panel represents the original data, the trend, the daily seasonality, the weekly seasonality, and the remainder respectively.
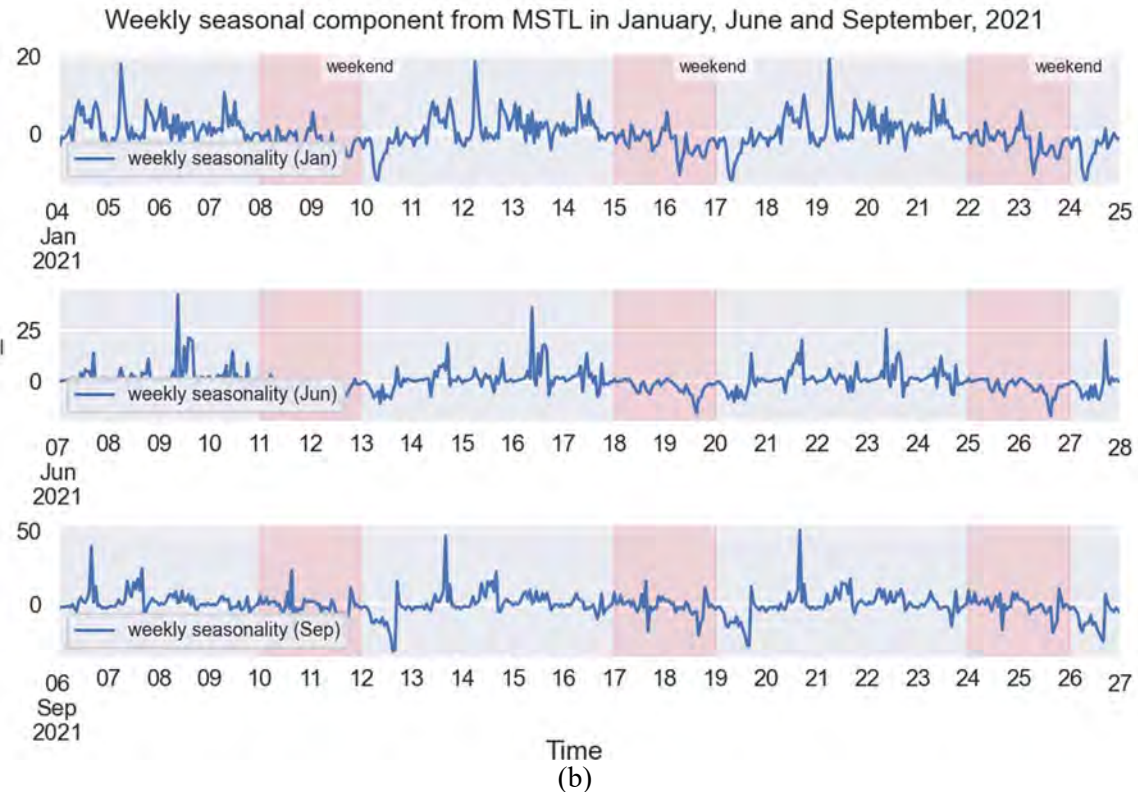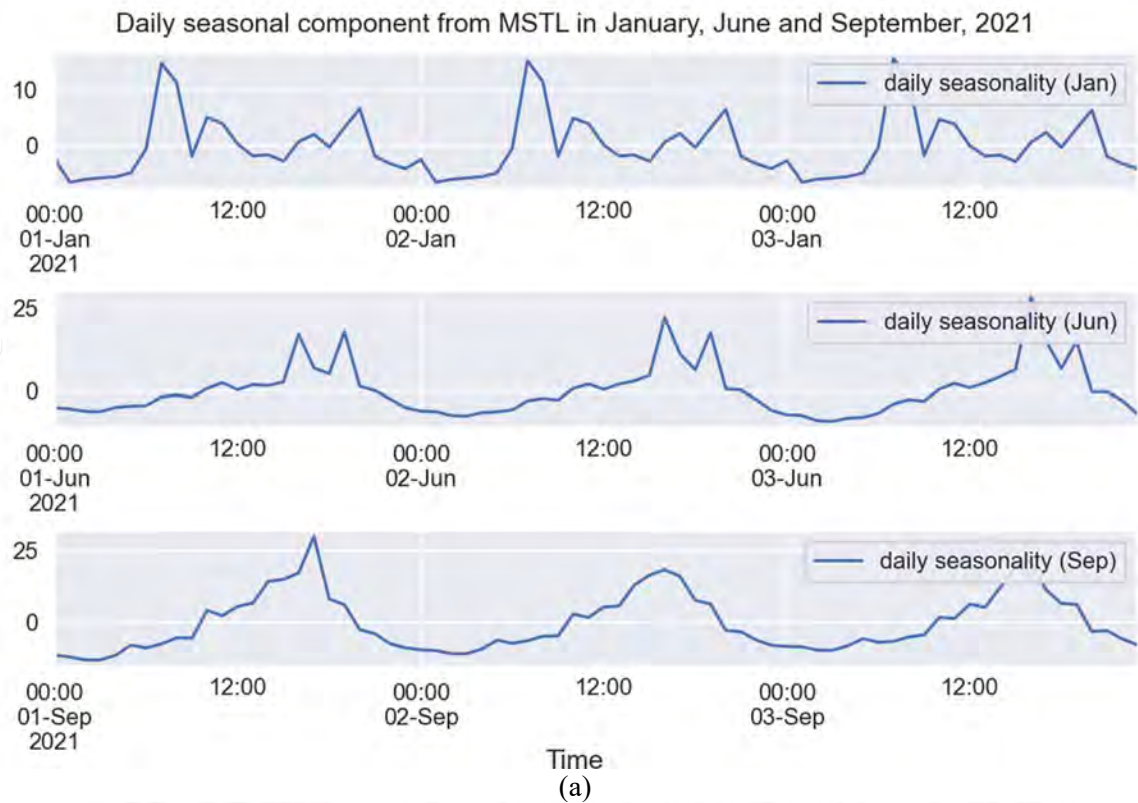
Figure 31. (a) Three-day snapshot of the daily seasonal component in January, June, and September 2021. (b) Three-week snapshot of the weekly seasonal component in January, June, and September 2021.